*Pure & Appl. Chem.*, Vol. 57, No. 11, pp. 1563–1588, 1985.
Printed in Great Britain.


# Spectroscopic investigation of local molecular dynamics in liquid crystal polymers

Lucien Monnerie

Laboratoire de Physicochimie Structurale et Macromoléculaire,
Ecole Supérieure de Physique et Chimie Industrielles de la Ville de Paris,
10, rue Vauquelin, 75231 PARIS Cedex 05 (France)

Abstract - Local motions in main-chain or side-chain liquid crystal polymers can be investigated using the same spectroscopic techniques which are applied to isotropic systems of small molecules or polymers. This paper deals with $^{1}H$, $^{13}C$ N.M.R., E.S.R. and dielectric relaxation. After recalling the specific characteristics of the most frequent liquid crystal phases, the type of information which can be obtained from each spectroscopic technique is indicated. The particular features related to the oriented nature of the liquid crystal phases are developed and illustrated with a few examples on small molecule systems. For liquid crystal polymers, specific problems due to the polymeric nature and the occurrence of glass-rubber transitions in addition to liquid crystal phase transitions are discussed. Finally, a few experimental results already obtained on dynamics of liquid crystal polymers are presented.

## I INTRODUCTION

Development of thermotropic liquid crystal polymers as either self-reinforced polymeric materials or materials for electronics displays and non-linear optics, requires a good knowledge of the local molecular motions in these polymers. Indeed, it is well-known from the behaviours of usual polymers that mechanical or dielectrical properties depend on the occurrence of transitions arising from side-chain or main-chain motions.

Though a complete understanding of molecular dynamics of bulk polymers has not yet been achieved, during the last years spectroscopic techniques have led to a great improvement in the description of molecular motions of polymers. So, it is reasonable to think that they will largely contribute to the analysis of local dynamics in liquid crystal polymers, although very few experiments have already been performed.

In this paper, we first recall some characteristic features of the most frequent liquid crystal phases. Then we describe what type of information on orientational order and dynamics can be obtained from each spectroscopic technique : $^{1}H$ and $^{13}C$ nuclear magnetic relaxation, electron spin relaxation and dielectric relaxation (D-N.M.R. is treated in the paper by H.W. Spiess). Emphasis is given to the range of motion correlation times which can be investigated by each method, we also point out the specific treatments which are required in the case of liquid crystal phases. Typical examples chosen among the studies performed on small molecule liquid crystals are discussed. The specific problems related to the long chain nature of the liquid crystal polymers are pointed out : difficulty to obtain single domain samples, easy supercooling leading to ordered glassy state, the occurence of a glass-rubber transition in addition to the mesophase transitions. Finally, the results already obtained on these polymers using the considered spectroscopic techniques are presented.

## II STRUCTURE AND ORIENTATION BEHAVIOUR OF MESOPHASES

### II.1 Structures of mesophases

Thermotropic molecules can be organized in different ways, leading to characterictic structures of mesophases. At high temperatures, an isotropic liquid state is achieved, unless chemical degradation occurs. At lower temperatures, various types of mesophases can be observed, depending on the chemical structure of the investigated compounds : a nematic phase (N) and different smectic phases(S). It is out of the scope of this paper to describe the various structures, detailed descriptions can be found in (Ref. 1 and 2).

#### *(a) Nematic*

In the ordinary nematic structure, there is a long range orientational order of the molecular long axes. The average direction of these long axes defines the director $\vec{n}$ which may be

treated as a vector, both directions of which + $\vec{n}$ and - $\vec{n}$ are equivalent. In most of cases, the ordinary nematic structure shows an optically positive uniaxial behaviour.

It is worth to notice that liquid crystals in the nematic phase possess a relatively low viscosity.

### *(b) Smectic A*

In smectic A phases, the molecules are parallel to one another and are arranged in layers, with the molecular long axes perpendicular to the planes of the layers. Within each layer, the lateral distribution of the molecules is random. The $S_A$ phase exhibits an optically positive uniaxial behaviour.

Though the overall viscosity of $S_A$ phases is much higher than that of N phases, the molecules within the layers have a relatively high mobility.

### *(c) Smectic C*

The structure of the $S_C$ phase is the tilted analogue of the $S_A$ phase. Indeed, the molecules are arranged in layers, but with the molecular long axes tilted to the layer normals. The centres of gravity of the molecules are ordered at random, and the molecules have a high mobility within the layers. The layers are free to slide over one another, i.e. there is no long range correlation, except of tilt direction, between the layers. The $S_C$ phases are optically biaxial.

### *(d) Smectic B*

In $S_B$ phase, the molecules are arranged in layers, with the molecular long axes perpendicular to the planes of the layers, as in $S_A$ phase, but the molecular centers in layers are positioned in a hexagonally close-packed array. There is long range hexagonal order within the layers and some correlations between the layers. Nevertheless, the molecules are still able to rotate quite rapidly about their long axis however, due to the hexagonal net dimension, the rotation has to be of a co-operative nature.

Contrary to the previously described phases which have a liquid-like behaviour, the $S_B$ phase is structurally solid-like though it exhibits shear and flow properties under stress.

### *(e) Smectic F*

In the $S_F$, the molecules are packed in layers with their long axes tilted with respect to the layer planes, the tilt angle may be 20°. The molecular packing in the layers is hexagonal. Within the layers a correlation length of 20-30 molecules exists but there is a poor correlation between the layers.

### *(f) Temperature occurrence of the various phases*

It has been observed, that the above mentioned phases appear in the following order when the temperature is decreased from the isotropic liquid state

$$I \rightarrow N \rightarrow S_A \rightarrow S_C \rightarrow S_F \rightarrow S_B$$

For the five considered mesophases. All variants of polymorphism observed in reality can be derived from this order by cancelling one phase or several phases, depending on the chemical structure of the investigated compound.

## II.2 Orientational order parameter – ordering potential

### *(a) Nematic phases*

In nematic phases, the average direction of orientation of the molecular long axes for the population of molecules defines the director $\vec{n}$ which may be treated as a vector, both directions of which + $\vec{n}$ and - $\vec{n}$ are equivalent.

The reference frame ($x_4$, $y_4$, $z_4$) associated to the mesophase is chosen so that the $z_4$ axis lies along the director n.

If the liquid crystal molecules are considered as rod-like molecules, the degree of parallel order of the individual molecular long axis, $z_2$, is described by a single orientational order parameter :

$$S_{z_2z_4} = \langle 3 \cos^2 \beta - 1 \rangle / 2 = \overline{P}_2$$

where $\beta$ is the angle between the individual molecular long axis and the director n, the brackets indicate a thermal average and $P_2$ is the second-Legendre polynomial.

In practice, liquid crystal molecules are not axially symmetric, but they have an oblong structure leading to a blade-like shape in such a way that the two coordinate axes of the molecular frame normal to the long axis would have different order parameters with respect to the director frame. The orientational order of the molecule would have to be described by a tensor with three principal values. $S_{x_2x_4}$, $S_{y_2y_4}$, $S_{z_2z_4}$. As $\sum_{ii} S_{ii} = 0$, the order and its symmetry are well described by only $S_{z_2z_4}$ and $\Delta = S_{x_2x_4} - S_{y_2y_4}$.

Due to the long range orientation correlation which characterizes the nematic phases, individual molecules are submitted to an ordering potential, U, arising from the surrounding molecules. In order to express this potential we have to consider the rotations from the molecular axis system ($x_2$, $y_2$, $z_2$) into the director axis system ($x_4$, $y_4$, $z_4$) defined by Euler angles $\Omega = (\alpha, \beta, \gamma)$, defined in Fig. 1.

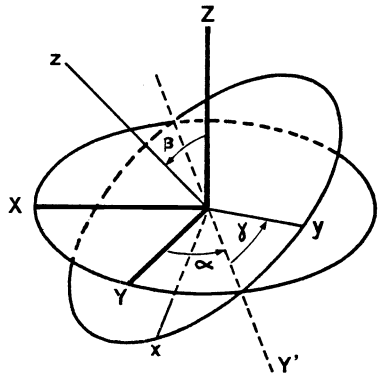


Fig. 1. Rotational transformation of the original frame (X, Y, Z) to a new axis system (x, y, z) through Euler angles ($\alpha$, $\beta$, $\gamma$)

For rod-like molecules, the general ordering potential is of form :

$$U(\Omega) = \sum_{p=1}^{\infty} \gamma_{2p} \cos^{2p} \beta$$

in practice, it appears that the higher order terms ($p > 2$) are negligeable, leading to :

$$U(\Omega) = \gamma_2 \cos^2\beta + \gamma_4 \cos^4\beta$$

where $\beta$ is the angle between the molecular $z_2$ axis and the director. The first term corresponds to the Maier-Saupe potential (Ref. 3).

For blade-like molecules, in which the molecular $x_2$ and $y_2$ axes are aligned to different extents, a non-axially symmetric ordering potential has to be considered :

$$U(\Omega) = \gamma_2 \cos^2\beta + \varepsilon \sin^2\beta \cos^2\alpha$$

If one chooses the $z_2$ axis as the molecular long axis which tends to align to a greater degree parallel to the director than both the $x_2$ and $y_2$ axes, one should have $|\gamma_2| > |\varepsilon|$ . $\varepsilon$ is proportional to the difference in the ordering parameters for the $y_2$ and $x_2$ axes and the case $\varepsilon < 0$ corresponds to the $y_2$ axis being ordered preferential to the $x_2$ axis along the director.

### *(b) Uniaxial smectic phases*

In the case of smectic phases, in addition to the long range orientation correlation, there is some translational order due to the layer structure. However, for the spectroscopic techniques which are considered in this paper, only the orientational behaviour is of interest.

For the considered uniaxial smectic phases, $S_A$ and $S_B$, the above expressions for the order parameters and the restoring potential can be used.

## II.3 Orientation of mesophases

Though liquid crystal phases are characterized by long range orientation order, nevertheless this order does not usually extend over the whole sample. Liquid-crystal samples are constituted by domains the director, $\vec{n}$, of which varies from one domain to another. This organization in domains yields the typical and frequently beautiful pictures observed in optical microscope between cross polarizers.

In order to develop electrooptic devices taking advantage of the change of optical properties of liquid crystals under electric fields, it is required to get single domain samples by inducing a bulk alignment. We will see later that single domain samples also are very useful to investigate the dynamic behaviour of liquid crystal phases.

The alignment is defined relatively to the substrate, the most important orientations are

- homeotropic alignment : $\vec{n}$ is perpendicular to the substrate
- planar alignment : $\vec{n}$ is in the plane of the substrate and lies along a given direction.

### *(a) Orientation of nematic phases*

Due to the very low viscosity of nematic phases, they are the easiest to orient. Single domain samples of nematic phases can be obtained using different orientation techniques :

- Treatment of substrate surface

The anchoring properties of liquid crystals in contact with a solid substrate can induce a well defined alignment (for a review article, see Ref. 4).

Thus, homeotropic alignment can be reached on a glass plate previously treated by surfactant molecules with a hydrophylic head sticking to the polar substrate and a hydrophobic tail pointing away, in order to reduce the surface energy.

Planar alignment are obtained, for example, with a substrate on which a vacuum deposition of a thin film (Au or $SiO_x$) has been performed under oblique incidence.

It has to be pointed out that to keep in the bulk the alignment due to the anchoring effects, the sample thickness should be smaller than about 100 µm.

- Magnetic field

Liquid crystal molecules have an anisotropic diamagnetic susceptibility in such a way that in a sufficiently strong magnetic field they are oriented and directed along one principal axis as determined by the direction of the field. More detailed information can be found in (Chap. 4 of Ref. 5) and (Ref. 6).

It is worthwhile to notice that magnetic alignment studies leads to determinations of the elastic constants $K_i$ of the three elastic mode distorsions of nematic phases (splay, bend, twist).

For most of small molecule liquid crystals, magnetic alignment can be obtained with magnetic fields ranging from 0.3 T to 2.1 T. The alignment temperature is chosen close to the clearing temperature in order to get the lowest viscosity of the nematic phase.

- Electric field

Nematic phases exhibit an anisotropy of both conductivity and dielectric constant.

When d.c. electric fields or low-frequency a.c. electric fields are applied, electrohydrodynamic phenomena occur yielding instabilities which give rise to either regular (Williams domain) or completely irregular domains. In such conditions no homogeneous alignment of the sample can be achieved.

Above a certain "cut off" frequency, the charges involved in the conductive regime do not have time to flow during one cycle and the instabilities disappear. In high frequency electric fields (typically 10 KHz), molecular alignment becomes purely dependent upon dielectric anisotropy.

Complementary information on the effect of electric fields on nematic phases are given in (Chap. 4, Ref. 5) and (Ref. 6 - 8).

### *(b) Orientation of smectic phases*

Due to the structure of smectic phases, they have a much higher viscosity and oriented single domain samples are difficult (sometimes impossible) to obtain.

If a nematic phase exists at higher temperature, the following procedure can be applied. The sample is first heated to the nematic phase in a magnetic field (0.3 to 2.1 T) in order to align the director parallel to the magnetic field. Then the sample temperature is slowly and carefully lowered until the smectic phase is formed. This procedure is cycled a few times near the nematic-smectic transition region. In the same way, a careful lowering of the sample temperature can retain the alignment from a $S_A$ to $S_B$ phase.

In the case of $S_C$ phase, alignment can be obtained by the same procedure but applying to the N phase a strong magnetic field oriented in the range of $45 \pm 15°$ relative to the normal to the glass plate. The smectic layers in these samples lie parallel to the glass plate, while the director is in the plane determined by the normal to the plate and the orientation of the field.

### *(c) Application of magnetic and electric fields*

In order to get more information on the dynamic behaviour of liquid crystals, it is frequently useful to perform spectroscopic measurements at different angles between the director and the applied magnetic or electric field. This implies that the director orientation can be kept constant, what is achieved using an equipment or a specially designed cell where a second field (electric or magnetic respectively), oriented along the sample director, is maintained during the measurements. Thus, for example, ESR or NMR studies are performed on samples the orientation of which is preserved by an electric field. Similarly, dielectric relaxation can be carried out with the sample in a magnetic field.

# III SPECTROSCOPIC METHODS FOR STUDYING DYNAMICS OF LIQUID CRYSTALS

Most of the spectroscopic techniques used to study the dynamics of isotropic system can be applied to the liquid crystal phases in spite of their ordered structure.

Depending on the considered mesophase the molecular dynamics of these systems covers the range from liquid state (motion frequency higher than $10^6$ Hz) to solid state. For this reason we will describe relaxation techniques which refer to liquid or solid state.

As previously stated, we will exclusively deal with $^1H$ and $^{13}C$ N.M.R., E.S.R. and dielectric relaxation.

## III.1 General information on the considered spectroscopic techniques

The purpose of this part is only to recall what type of information (order parameter, dynamics) can be obtained from each technique and what motion frequency range can be investigated. In each case, references to specialized books or review articles are given for the reader interested in detailed theoretical or technical information.

### *(a) $^1H$ N.M.R. (for details see ref. 9)*

First of all, if one considers in a molecule a pair of protons, $H_1$ - $H_2$, separated by a distance d, the measurement of the splitting, $\Delta\nu$, between the two lines due to the dipolar coupling between the nuclear magnetic moments leads to the orientational order parameter of the considered H - H vector.

For real molecules, due to the increased number of protons, the number of dipolar coupling so does and the spectrum becomes very complex. The measurement of order parameters from $^1H$ NMR requires that protons in some specific positions can be replaced by deuterons. For example, with the partially deuterated MBBA molecule :

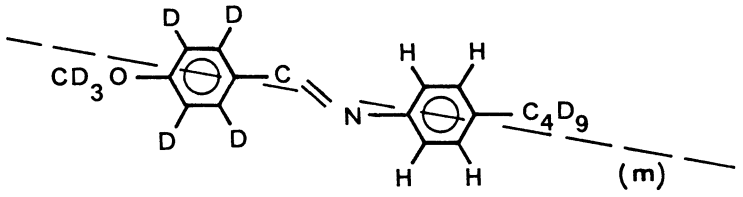


the internuclear vector for the ortho protons is almost parallel to the molecular long inertial axis (m), whereas the vector for the meta protons is almost perpendicular and that for the para protons is at an angle of about 60°. Thus, $^1H$ NMR allows to determine the order parameters for these different vectors and to test the axially symmetric behaviour of the molecule.

Detailed information on molecular dynamics from NMR is obtained from magnetic relaxation experiments.

First, for mobile systems, one can measure the longitudinal relaxation of the total magnetization (also called spin-lattice relaxation), characterized by a relaxation time $T_1$. In order to be effective on $T_1$ the molecular motions have to get a frequency around the Larmor frequency of the considered protons. Thus, depending on the applied magnetic field, it corresponds to motion correlation times in the range $2.10^{-12}$ s to $10^{-5}$ s. Another macroscopic relaxation time, $T_2$, deals with the transverse relaxation of the total magnetization (also called spin-spin relaxation). $T_2$ values are affected by the same molecular motions as $T_1$ but, in addition, the low frequency motions take part. It has to be recalled that $T_2$ is inversely proportional to the line width.

Dealing with a lower frequency range, the longitudinal relaxation time in the rotating frame, $T_{1\rho}$, corresponds to motions with correlation times in the range $10^{-4}$ s - $10^{-6}$ s.

Due to the $r^{-6}$ dependence of the relaxation times, most of the intramolecular contributions will correspond to 2 protons bonded to the same C or bonded to 2 adjacent C. However, when applying $^1H$ N.M.R. to study the dynamics of molecules in condensed state, in addition to the intramolecular reorientation contribution to the relaxation processes, there is a contribution coming from intermolecular H - H interactions. These interactions are related to self diffusion translation motions of molecules, changing the H - H intermolecular distance. The molecular description involves the molecular translation diffusion coefficient, D, and the distance, d, of closest proton approach of neighbouring molecules.

It has to be pointed out that the intramolecular and intermolecular contributions can be separated by performing $T_1$ or $T_{1\rho}$ measurements on protonated molecules diluted at various concentrations in perdeuterated molecules

### (b) $^{13}C$ N.M.R. (for details see refs. 9–12)

$^{13}C$ is naturally present in the skeleton of molecules but, because its low isotropic abundance (~ 1 %) there is no dipolar coupling between $^{13}C$ spins. However, there remains a dipolar coupling with proton spins.

The magnetic relaxation times will involve the orientational motions of the vectors between one $^{13}C$ and the bounded protons exclusively, all the other protons being to far to efficiently contribute. In particular, there is no intermolecular contributions, contrary to $^{1}H$ N.M.R.

The main interest of $^{13}C$ N.M.R. studies is that the resonance lines of the different C atoms of a molecule are usually sufficiently well separated and thus the orientational motion of a specific C - H bond can be studied.

In the liquid range (high frequency motions) the $T_1$ and $T_2$ relaxation times can be measured. The correlation times of the molecular motions which are effective range from $5.10^{-12}$ s to $10^{-8}$ s depending on the value of the applied magnetic field.

In the range of lower frequency motions occuring either in liquids or solids, $T_{1\rho}$ measurements reflect motions with correlation times from $10^{-4}$ s to $10^{-6}$ s.

In this frequency range, another interesting information comes from the high chemical shift anisotropy observed for $^{13}C$ lines. Indeed, the shape of the line depends on the averaging of the chemical shift anisotropy tensor by the molecular motions, however to get a significant effect it requires correlation times shorter than $10^{-4}$ s. Another interesting information which can be obtained from the measurement of the chemical anisotropy is the orientational order parameter of the molecular long axis.

Finally, in some cases, information on dynamics may arise from the aspect of the $^{13}C$ spectrum. It deals with chemical exchange and corresponds to the fact that $^{13}C$ sites of a molecule which would be inequivalent in a rigid lattice (and would result in different lines) can become equivalent if molecular motions occur (leading to a single line). The aspect of the spectrum is strongly dependent on the frequency of the motion in the range $10^{-1}$ Hz to $10^{-6}$ Hz.

From above considerations, it is clear that $^{13}C$ N.M.R. provides a very powerful tool to investigate molecular dynamics. In addition to measurements on liquid systems, it can be now applied to solid samples using the high-resolution solid state N.M.R. equipments commercially available.

### (c) E.S.R. (for details see refs. 14–17)

Contrary to $^{1}H$ and $^{13}C$ N.M.R., the studies of molecular dynamics with E.S.R. require the use of a free radical probe. In most cases, a nitroxide group is used, due to the high stability of this radical. The various nitroxide probes which are considered in this paper are listed in Table 1. In nitroxide radicals, the odd electron is largely confined to a 2 $p\pi$ atomic orbital on nitrogen and the magnetic axes which diagonalize the $\bar{g}$ and $\bar{A}$ tensors are shown in Fig. 2.

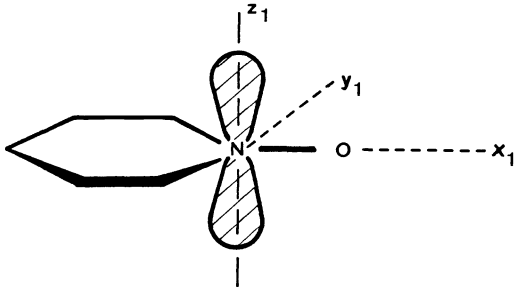


Fig. 2. Magnetic axes of a nitroxide radical and representation of the 2p$\pi$ atomic orbital of nitrogen

The hyperfine coupling of the free electron with the I = 1 nuclear spin of nitrogen leads to three transitions and an E.S.R. spectrum with three lines. The hyperfine coupling depends on the orientation of the magnetic axes relatively to the applied magnetic field. If the nitroxide group undergoes a motion, the hyperfine coupling will be modulated. However, due to the rather large value of this coupling, only motions with correlation times, $\tau$, shorter than $10^{-8}$ s can have an efficient averaging effect.

As shown in Fig. 3, the E.S.R. spectra can have very different aspects, depending on the mobility of the nitroxide group. At high mobility ($\tau < 10^{-9}$ s) a well resolved spectrum with three lines is observed, whereas for a powder sample where the nitroxide molecules may get any orientations, an almost structureless spectrum is recorded. For intermediate mobilities, the line width of each line can be measured and the corresponding correlation time is derived (similarly to N.M.R., the line width is inversely proportional to $T_2$). In the correlation time range, $10^{-9}$ s $< \tau <$ $5.10^{-8}$ s, simulation of the spectrum has to be performed to obtain

TABLE 1. Acronyms and formula of the nitroxide probe considered in this paper

| Acronym | Formula |
|---|---|
| Tempol | 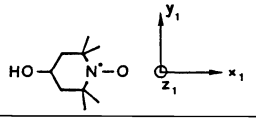 |
| P.D. Tempone | 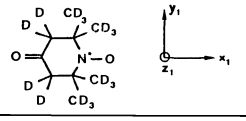 |
| P-Probe | 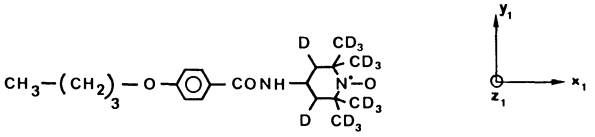 |
| CSL |  |

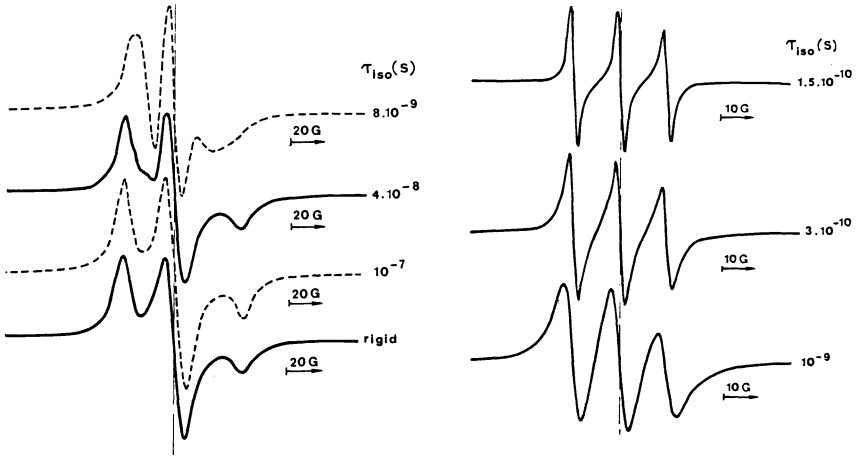


Fig. 3. Typical E.S.R. spectra of a nitroxide probe in an isotropic medium. The corresponding correlation times of the isotropic motion of the probe are indicated

τ, a computer program is listed in (Ref. 14, Chap. 3).

As the E.S.R. spectrum depends on the orientation of the nitroxide group relatively to the applied magnetic field, it yields a possibility to measure its orientational order parameter. Thus, for a single domain liquid crystal sample, E.S.R. spectrum recorded with the magnetic field parallel (or perpendicular) to the director yields a determination of the order parameters of the nitroxide magnetic axes relatively to the applied magnetic field (Ref. 14, Chap. 10). If the nitroxide group is covalently bound to other chemical group in the probe molecule, the order parameter of a given molecular axis of the probe can be deduced from the measured order parameter if the angle between the two considered axes is known.

It has to be noticed that the order parameter which is so determined concerns the nitroxide molecule put in the liquid crystal and not the liquid crystal molecules themselves. This is an important point, which will be later illustrated, because depending on the chemical structure and the shape of the nitroxide probe, it can be located either close to the rigid core of the liquid crystal molecules or in the region of the flexible tails.

### *(d) Dielectric relaxation (for details see refs. 18–22)*

Molecules with a permanent dipole moment respond to an electrical field such that when an external electric field is applied, the interaction between the electric field and the dipole moment changes the probability distribution of the orientation of the molecules.

Let us first consider the behaviour of a dipole system in a static electric field. The static permittivity, $\varepsilon^o$, can be calculated considering the instantaneous dipole moment $\vec{M}(0)$ of a sphere of volume V, the resulting expression is :

$$\varepsilon^o - \varepsilon^\infty = (4\pi/3\ kT)\{3\ \varepsilon^o(2\ \varepsilon^o + \varepsilon^\infty)/(2\ \varepsilon^o + 1)^2\}<\vec{M}(0).\vec{M}(0)>\ V^{-1}$$

where $\varepsilon^\infty$ is the limiting high frequency permittivity, given by : $\varepsilon^\infty = n_o^2 + \Delta\varepsilon_{ir}$ where $n_o$ is the optical refractive index and $\Delta\varepsilon_{ir}$ is the contribution from the infra-red polarizability of molecules, and $< \vec{M}(0).\vec{M}(0) >$ is the mean-square dipole moment of the sphere averaged over all configurations of the contained molecules. If $n_m$ is the number of molecules per unit volume and $< P^2 >$ is the mean-square dipole moment of a molecule, one obtains the following relation

$$< \vec{M}(0) . \vec{M}(0) > = V\ n_m < P^2 > g_1$$

where $g_1 = 1 + \sum_{i \neq 1} < \vec{P}_1(0) . \vec{P}_i(0) >/< P^2 >$

1 refers to any given reference molecule and i to other molecules. This $g_1$ term expresses the vector correlations between the dipolar molecules. It can be determined from $\varepsilon^o$, $\varepsilon^\infty$ measurements using the dipole moment value of the individual molecules determined from studies on small molecule glass-forming systems in which the dipolar solute is at low concentration, indeed in this case $g_1 \simeq 1$.

Such a calculation as been extended to small molecule liquid crystal nematic phase (Ref. 23, 24) considering the static permittivities ($\varepsilon^o_\parallel$, $\varepsilon^o_\perp$) and high frequency permittivities ($\varepsilon^\infty_\parallel$, $\varepsilon^\infty_\perp$) corresponding to electric field parallel or perpendicular to the director. The resulting expression involves the orientational order parameter S, the longitudinal and transverse components of the molecule dipole moment and the molecule polarizability tensor, the lengths of the long and short axes of the ellipsoidal molecule and $g_\parallel$, $g_\perp$ describing the molecule dipole correlations parallel or perpendicular to the director. Although the dielectric anisotropy, $\Delta\varepsilon = \varepsilon_\parallel - \varepsilon_\perp$, contains the order parameter, this information cannot be derived from this measurement. On the contrary, if S is determined by another technique and the involved molecular quantities are known, the $g_\parallel$ and $g_\perp$ factors can be obtained.

When dealing with isotropic systems of polymer chains instead of small molecule isotropic systems, the $g_1$ term becomes important, even if the cross-correlation terms between different chains is ignored. Indeed, for a polymer chain with dipolar units, there is an angular correlation between the dipolar groups along each chain. For polymers constituted with repeat units of dipole moment $\mu$ :

$$< \vec{M}(0) . \vec{M}(0) > = V\ n_u\ \mu^2(1 + \sum_{k' \neq k} < \vec{\mu}_k(0) . \vec{\mu}_{k'}(0) >/\mu^2)$$

where $n_u$ is the number of dipole units per unit volume, $\vec{\mu}_k(0)$ is the instantaneous dipole moment of a given reference unit, k, and $\vec{\mu}_{k'}(0)$ is the similar quantity for a different unit k' along the same chain as the unit k. Although the cross-correlation terms decrease when $|k' - k|$ is increased, nearest neighbours and next-nearest neighbours may have substantial contributions.

Information on dynamic behaviour of dipolar groups are provided by the frequency dependence of the complex dielectric permittivity, $\varepsilon^*(\omega)$. This quantity can be expressed using the time-frequency Fourier transform relation involving the time-correlation function of the instantaneous dipole moment :

$$p(\omega)(\varepsilon^*(\omega) - \varepsilon^\infty)/(\varepsilon^o - \varepsilon^\infty) = 1 - i\omega \int_o^\infty \phi(t)\ \exp(-i\omega t)dt$$

$$\phi(t) = < \vec{M}(0) . \vec{M}(t) >/ < \vec{M}(0) . \vec{M}(0) >$$

and $p(\omega)$ is an internal field correction, which, for dilute solution is approximately equal to unity, and is assumed to be equal to unity for pure substances.

The real and imaginery parts of the complex permittivity are usually denoted as $\varepsilon'(\omega)$ and $\varepsilon''(\omega)$ respectively. $\varepsilon'(\omega)$ corresponds to the in-phase response and is associated with the recoverable energy, whereas $\varepsilon''(\omega)$ is the quadrature response related to the energy dissipated by dipole motions.

For isotropic systems of small molecules, each of them with a dipole moment, $\vec{\mu}$, the cross-correlation terms describing the correlation of motions of different molecules are generally ignored and only the orientational autocorrelation function is considered :

$$\phi(t) = < \vec{\mu}(0) . \vec{\mu}(t) >/\mu^2$$

The expression of $\phi(t)$ depends on the motional model considered. In the simplest case of an

isotropic reorientation process (Debye relaxation) characterized by an exponential autocorrelation function with a relaxation time, $\tau$, it leads to :

$$(\varepsilon'(\omega) - \varepsilon^{\infty})/(\varepsilon^{o} - \varepsilon^{\infty}) = 1/(1 + \omega^2 \tau^2)$$

$$(\varepsilon''(\omega))/(\varepsilon^{o} - \varepsilon^{\infty}) = \omega\tau/(1 + \omega^2 \tau^2)$$

Typical curves for $\varepsilon', \varepsilon''$ as a function of $\omega$ are shown in Fig. 4. The maximum of $\varepsilon''$ occurs at the frequency associated with the characteristic correlation time : $\omega_m = 2\pi\nu_m = \tau^{-1}$.

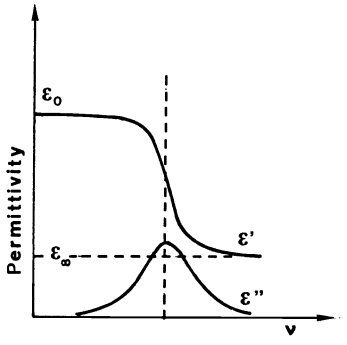


Fig. 4. Schematic representation of the frequency dependence of dielectric permettivity components, $\varepsilon'$ and $\varepsilon''$ in the case of a single relaxation time.

If the molecule undergoes several types of motions characterized by sufficiently different relaxation times, separate relaxation processes will be observed yielding a $\varepsilon''$ curve with different maxima, each of which corresponds to a given type of motion. Similarly, if a flexible molecule has, for example, two different polar groups which are able to undergo intramolecular reorientations at two sufficiently different frequencies, the $\varepsilon''$ curve would show two separate maxima corresponding to the change in the autocorrelation function of the total dipole moment of the molecule due to the occurrence of intramolecular motions of each dipolar group.

For the ordered phases of small molecule liquid crystals, dielectric relaxation experiments can be performed on single domain samples with the electric field oriented either parallel or perpendicular to the director. The autocorrelation functions of interest in this cases concern the parallel or perpendicular component ($\mu_{\parallel}$, $\mu_{\perp}$) of the dipole moment, respectively. $\mu_{\parallel}$ and $\mu_{\perp}$ are functions of the longitudinal and transverse components of the ellipsoidal molecule dipole moment.

Investigation of polymer chain dynamics by dielectric relaxation leads to consider the complete correlation function :

$$\phi(t) = \{ < \vec{\mu}_k(0) \cdot \vec{\mu}_k(t) > + \sum_{k' \neq k} < \vec{\mu}_k(0) \cdot \vec{\mu}_{k'}(t) > \} /$$

$$\{ < \vec{\mu}_k(0) \cdot \vec{\mu}_k(0) > + \sum_{k' \neq k} < \vec{\mu}_k(0) \cdot \vec{\mu}_{k'}(t) > \}$$

Whereas the static cross-correlation terms can be estimated from chain conformation statistics, it is not possible to evaluate the dynamic cross-correlation terms. However, it has been shown (Ref. 25) that if the autocorrelation function of a polymer unit, k, does not depend on the relative conformation of k and k' units, the time dependence for any cross-correlation term is the autocorrelation term of a unit in the chain. Thus, $\phi(t)$ takes the simple expression :

$$\phi(t) = < \vec{\mu}_k(0) \cdot \vec{\mu}_k(t) > / < \vec{\mu}_k(0) \cdot \vec{\mu}_k(0) >$$

Of course, the expression of $\phi(t)$ depends on the type of motional model considered.

All the above expressions clearly show that the frequency dependence of the dielectric permittivity involves the first order spherical harmonic functions, contrary to NMR and ESR which involve the second order spherical harmonic functions.

A great interest of dielectric relaxation deals with the large frequency range which can be explored. Whereas NMR and ESR have intrinsic limitations in the range of motion correlation times which are efficient on the involved relaxation, dielectric relaxation experiments have no intrinsic limitations. In practice, the high frequency range is limited by the available equipments to $30.10^9$ Hz, concerning the low frequency range, conductivity processes are frequently superposed to the relaxation behaviour below $10^4$ Hz, but they can be subtracted for their frequency dependence is well known. Thus, for liquids it is possible to get dynamics information down to 1 Hz. In the case of solids, where the conductivity contribution is very low, information on motions can be obtained down to $10^{-4}$ Hz. Consequently, a very broad frequency range is covered without any gap.

Finally, it is worth noting that when several dipolar groups are present in a molecule, even if separate dielectric relaxations are observed, there is no direct way for assigning a given relaxation to a specific polar group, it has to be done by a comparison with other techniques or by studying a set of molecules which chemical structure is gradually changed.

## III.2 Characteristic features of dynamic spectroscopic studies in liquid crystals

In all the above considered spectroscopic techniques, motions of the investigated molecules are measured through tensor quantities the values of which are changed by the rotation of the molecule relatively to the fixed laboratory frame. Thus, going from the coordinate system associated with the investigated quantity (dipole moment, nuclear vector, magnetic axes...) to the laboratory frame, we have to consider several intermediate systems. The rotation from one system to the other is defined by a set of Euler angles (Fig. 1). Successively, these reference systems are :

- the principal axis system, $F_1$, ($x_1$, $y_1$, $z_1$) associated to the involved quantities.
- the diffusional axis system of the molecule, $F_2$, which corresponds to the principal axes of the rotational diffusion tensor of the molecule. Usually, one assumes that the principal molecular axes for ordering are the same as for rotational diffusion. The transformation from $F_1$ to $F_2$ is defined by Euler angles $\textcircled{H}_1 = (\alpha_1, \beta_1, \gamma_1)$
- the instantaneous director system, $F_3$, which characterizes the orientational state, at a given time, of the surrounding of the investigated molecule. The $F_2 \rightarrow F_3$ transformation is described by $\textcircled{H}_2$
- the average director system, $F_4$, of a domain or of the sample if we deal with a single domain sample. Usually, this system is chosen so that the director lies along $z_4$. $F_3$ and $F_4$ are related through $\textcircled{H}_3$.
- the laboratory system, $F_5$. The transformation from $F_4$ to $F_5$ corresponds to $\textcircled{H}_4$.

The coordinate transformations $\textcircled{H}_i$ (i = 1 to 4) allow one to incorporate the time scales and amplitudes of the various physical motions which are implied in the dynamics of liquid crystal phases and affect the measurements performed in the laboratory system. This procedure has been applied for each considered spectroscopic technique, complete developments are given for N.M.R. and E.S.R. in (Ref. 26 and 27) and for dielectric relaxation in (Ref. 28).

In the present paper we will focus on the particular types of motions which are involved in each transformation.

### *(a) $F_1 \rightarrow F_2$ (principal axes to diffusional system)*

As liquid crystal molecules usually have some internal flexibility, the rotational diffusion axes correspond to the diffusion behaviour averaged over the various conformations of the molecules.

The $F_1 \rightarrow F_2$ transformation describes the intramolecular motions performed by the molecular group observed with the considered spectroscopic technique.

For example, if we consider the following molecule,

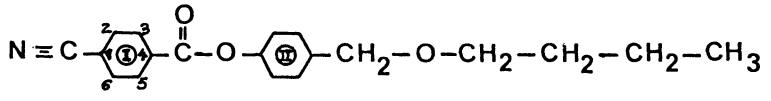

the $^{13}C$ NMR $T_1$ or $T_{1\rho}$ values of aromatic carbons 2, 3, 5, 6 will be affected by the rotation of the phenyl ring I around its $C_1 - C_4$ axis. Similarly, the rotation of the terminal $CH_3$ around the $CH_2 - CH_3$ bond or the trans-gauche conformational changes of the $CH_2$ groups may contribute to the relaxation of aliphatic carbons.

In dielectric measurements, the motion of the nitrile dipole will describe the intramolecular motion of the $C_1 - C_4$ axis of the phenyl ring I, whereas the $CH_2 - O - CH_2$ dipole will be related to the intramolecular motions associated with both the tail and the phenyl ring II.

In the case of ESR, the nitroxyde group, the orientational motion of which is observed, may get in some probe molecules (see Table I) an intramolecular motion, as for example in the P-probe. On the contrary, in CSL probe the nitroxyde group is rigidly fixed to the molecule, but the magnetic axes involved in the relaxation do not coincide with the rotation diffusion frame.

It has to be pointed out that all these intramolecular motions frequently occur in a high frequency range ($10^9 - 10^{11}$ Hz).

### (b) $F_2 \rightarrow F_3$ (diffusional system to instantaneous director)

This transformation corresponds to the rotational diffusion motion of a liquid crystal molecule relatively to the oriented surrounding molecules. The intramolecular motions performed by the various constituting groups lead to consider a mean shape of the overall molecule. It can be a rod or a blade. The complete description of the diffusion of a rigid blade requires 3 diffusion constants corresponding to rotation motions around the molecular long axis and the two different perpendicular axes. However, as the values of these two latter diffusion constants are close to each other, the diffusion motion is usually treated for a rigid rod-molecule. In this case, the characteristic diffusion coefficients are : $D_{\parallel}$ for the motion about the molecular long axis, $D_{\perp}$ for the motion about the perpendicular axis; the corresponding correlation times are $\tau_{R\parallel}$ and $\tau_{R\perp}$ respectively ($\tau_R = 1/(6\ D)$); importance of anisotropy is reflected by the anisotropy coefficient $N = D_{\parallel}/D_{\perp}$. Accurate determination of $D_{\parallel}$ and $D_{\perp}$ is sometimes difficult to reach from measurements and only a mean diffusion coefficient, $\bar{D} = (D_{\parallel} \cdot D_{\perp})^{1/2}$ and a mean correlation time, $\tau_{\bar{R}} = (\tau_{R\parallel}\ \tau_{R\perp})^{1/2}$ are frequently obtained.

In many cases, instead of considering the asymmetry shape of the molecule and the resulting anisotropic motion, the molecule is treated as a sphere and its rotational diffusion behaviour is an isotropic motion characterized by a single diffusion coefficient, $D_{is}$, and a single correlation time, $\tau_{is}$. Of course, such a crude approximation yields much simpler treatments.

The next step deals with the motional models which are used to describe the diffusion process of the molecule, independently of its shape. Several models have been developed, depending on the considered frequency range and the size of the molecule. For fast motions, i.e. $\tau < 10^{-9}$ s, one always considers a Brownian rotational diffusion which corresponds to an infenitesimal reorientation of the molecule with each collision with the surrounding molecules. For slower motions, in addition to this Brownian model which seems to fairly well account for the motion of bulky molecules, two other motional models are considered. The first one is the jump diffusion model, in which the molecule has a fixed orientation for the time $\tau$ and then jumps instantaneously to a new direction; the second one is the free diffusion, in which the molecule rotates freely for a time $\tau$ due to inertial motion and then reorients instantaneously to a new direction. These two latter models are satisfactory applied to small molecules, the motions of which are slown down by the high viscosity of the surrounding medium.

The above features concern molecular motions occuring both in isotropic medium and in ordered systems as liquid crystal phases. The situation is different when dealing with the type of restoring potential applied to the mobile molecule. Indeed, for ordinary liquids or polymers, an isotropic potential is considered, while for liquid crystal phases one has to use either an axially symmetric potential (rod-like molecule assumption) or a non-axially symmetric potential (blade-like molecule). The two cases have been treated for E.S.R. (Ref. 29 and 30).

It has to be noticed that the thermal averages of these fast molecular motions give the orientational order parameters, here above defined. Thus, the spectroscopic techniques applied to dynamics studies will also lead to a determination of the order parameters.

### (c) $F_3 \rightarrow F_4$ (instantaneous director to average director)

The diffusional molecular motions have been described relatively to the local surrounding which has a temporary order in the case of liquid crystal phases, leading to an instantaneous director. If we now look at what happens with time, this instantaneous local director undergoes orientation changes relatively to the average director, which is the same as the director of the domain.

The $F_3 \rightarrow F_4$ transformation accounts for these fluctuations of the instantaneous local director.

A first mechanism lies in orientation order director fluctuation (ODF), which are collective elastic fluctuations in the deformations of liquid crystals resulting from hydrodynamic effects (Ref. 31 and 32). These fluctuations can be analysed in relaxation modes with wavevec tor q corresponding to dimensions much greater than molecular dimensions. If one describes the distortion behaviour of the liquid crystal phase using a single elastic constant K (average of the three elastic constants $k_1$, $k_2$ and $k_3$) and an average viscosity $\eta$, the amplitude of the mode q waves is proportional to $kT/Kq$ and the relaxation time, $\tau_q$, which characterizes the highly damped, viscous relaxation of the waves is $\tau_q^{-1} = Kq^2/\eta$. A typical value for the fastest mode is $\sim 10^{-8}$ s, but the amplitude of these waves is very small, making them of low efficiency for dynamic measurements in this time range. This means that ODF will not affect E.S.R. or high magnetic field $T_1$ N.M.R. experiments but that they contribute to $T_{1\rho}$ N.M.R. or low magnetic field $T_1$ N.M.R., as well as dielectric relaxation studies at frequencies lower than $10^7$ Hz.

In the frequency range where the ODF mechanism efficiently contributes, a $\omega^{-1/2}$ frequency dependence of $T_1^{-1}$ is expected, characteristic of ODF. Furthermore $T_1^{-1}$ is proportional to $T\eta^{1/2}/K^{3/2}$.

Another mechanism, called slowly relaxing local structure, SRLS, has been proposed to account for the orientation changes of the local director (Ref. 30). Contrary to the ODF mechanism, which occurs at a scale much larger than the molecular dimensions, the SRLS model deals with processes on a molecular scale. Indeed, it considers that the motions of one molecule (as the ones above described) are performed in the cage of its neighbours, but because the constraints arising from the cage the correlation function does not go to zero. Due to the translational and rotational diffusion of the constituting molecules, the cage structure is slowly changed, leading to a complete averaging of the orientation of the considered molecule. A crude estimation of the relaxation time of this cage structure leads to values in the range $10^{-9}$ s to $3.10^{-8}$ s.Thus, this SRLS mechanism can efficiently contribute to the high frequency spectroscopic measurements.

### *(d) $F_4 \rightarrow F_5$ (average director to laboratory frame)*

For single domain liquid crystal samples, the transformation from the average director system to the laboratory frame is well defined. In many experiments, the sample is oriented in such a way that the director lies along the magnetic field. However, complementary useful information can be obtained changing the orientation of the director relatively to the magnetic field.

For multi-domain samples, the domains have different orientations in such a way that at the scale of a domain there is a local ordering but the whole sample appears macroscopically disordered. The $F_4 \rightarrow F_5$ transformation consequently implies an average over the domain orientation using an appropriate static distribution of the domain directors. As such a distribution is frequently unknown, the investigation of multi-domain samples is considerably more difficult than that of a single domain. Unfortunately, there is sometimes no other possibility, even with small molecule liquid crystals (as for example for some smectic phases).

## IV EXAMPLES OF DYNAMIC BEHAVIOUR IN SMALL MOLECULE LIQUID CRYSTALS

Applications of the considered spectroscopic techniques to investigation of molecular dynamic behaviour of liquid crystal phases will be first illustrated in the case of small molecules. Indeed, many studies have been performed on such systems and we will consider the most typical ones. The various molecules which will be considered below, are represented in Table 2.

### IV.1 $^1$H N.M.R.

$T_1$ measurements on a very broad frequency range (2 kHz - 270 MHz) using the field cycling technique in the low frequency domain, have been performed on MBBA in the nematic phase from 18°C to 45°C (Ref. 33). The dependence of $T_1$ on the angle between the magnetic field and the director is in agreement with ODF mechanism as the only relaxation process; indeed no angular dependence is expected for self-diffusion mechanism (SD). The frequency dependence of $T_1$ can be analysed considering 3 contributions : ODF, SD and reorientation motions of the molecule, R. Assuming that there is no cross-terms, the following expression is obtained :

$$T_1^{-1} = P_{ODF} \cdot T_1^{-1}(ODF) + P_{SD} \cdot T_1^{-1}(SD) + P_R \cdot T_1^{-1}(R)$$

$P_i$ represents the fraction of the 21 protons per molecule concerned by the i mechanism. So, due to the high flexibility of the MBBA side chains, the ODF mechanism is most probably restricted to nearest neighbours of the 8 ring protons, $P_{ODF} = 8/21$. On the contrary, all the protons participate to the SD process and $P_{SD} = 1$. Concerning the rotation mechanism, the motion around the molecular long axis is very rapid and does not contribute (neither the $CH_2$ and $CH_3$ intramolecular motions do), the rotation around the perpendicular axis is the only one to participate. The fit of the experimental curves with such a decomposition leads to the results shown in Fig. 5 , and to the values of the interesting molecular quantities reported on Table 3. The activation energy associated to the self-diffusion process, $E_{SD} = 37$ KJ.mole$^{-1}$, and the very small preexponential factor, $D_o = 0.34$ cm$^2$.s$^{-1}$, suggest some kind of cooperative diffusion motion. At high temperature only the rotation about the perpendicular axis takes part in the relaxation. ODF is the dominant relaxation mechanism at low frequencies, up to about $10^5$ Hz, what could be expected from the involved hydrodynamic fluctuations.

TABLE 2 - Acronyms and formula of considered liquid crystal molecules.

| Acronym | Formula |
|---|---|
| MBBA | 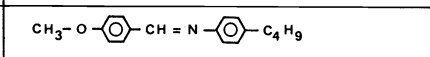 |
| TBBA | 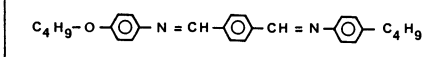 |
| 40 - 6 | 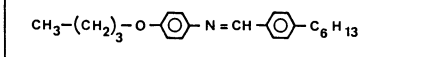 |
| 50 - 6 | 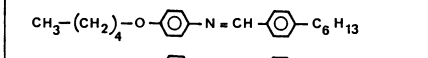 |
| 50 - 7 | 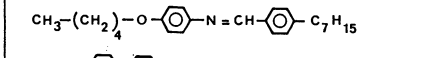 |
| 5 CB | 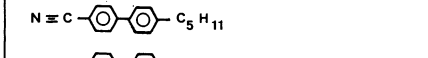 |
| 7 CB | 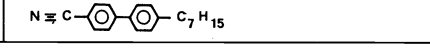 |

TABLE 3 - Characteristic parameters of the self-diffusion and rotation model of nematic MBBA, from $^1$H N.M.R..

| T(K) | τ(SD) (S) | D(SD) ($cm^2.s^{-1}$) | d (Å) | $\tau_R$ |
|---|---|---|---|---|
| 291 | $1.21.10^{-9}$ | $0.98.10^{-7}$ | 2.67 | $2.43.10^{-7}$ |
| 300 | $0.65.10^{-9}$ | $1.78.10^{-7}$ | 2.64 | $1.45.10^{-7}$ |
| 308 | $0.50.10^{-9}$ | $2.27.10^{-7}$ | 2.61 | $0.94.10^{-7}$ |
| 318 | $0.30.10^{-9}$ | $3.47.10^{-7}$ | 2.50 | $0.57.10^{-7}$ |

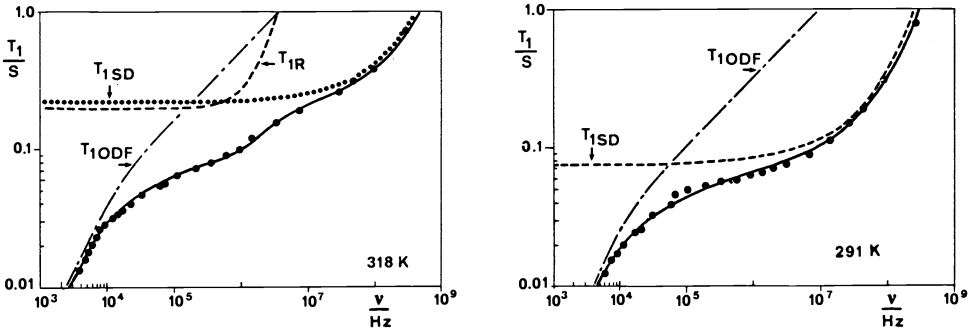


Fig. 5. $T_1$ values and $T_{1ODF}$, $T_{1SD}$, $T_{1R}$ contributions for MBBA at 291 K and 318 K (After Ref. 33)

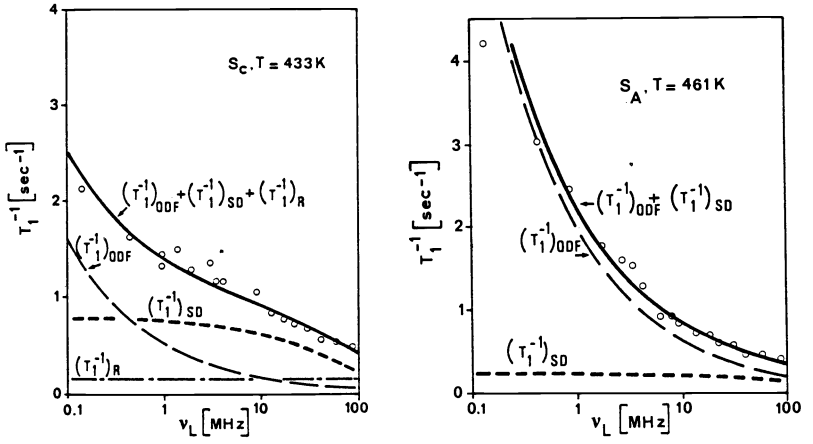


Fig. 6. $T_1$ proton spin relaxation dispersion in $S_A$ and $S_C$ phases of TBBA. (After Ref. 34)

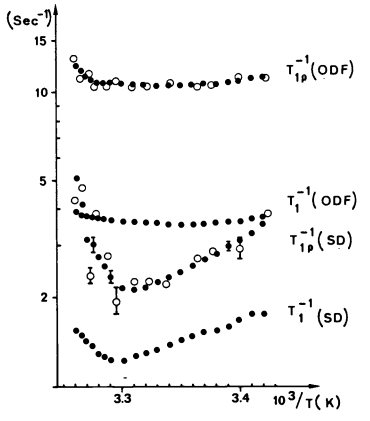


Fig. 7. Intermolecular (SD) and intramolecular (ODF) contributions to the $T_1$ and $T_{1\rho}$ relaxation times vs. $10^3/T$ for 5CB. (After Ref. 35).

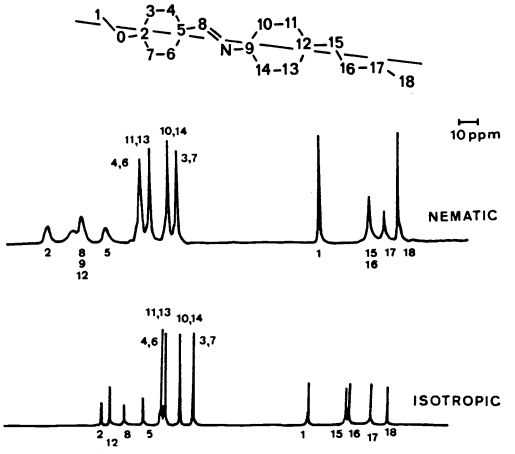


Fig. 8. $^{13}C$ N.M.R. spectra of MBBA.

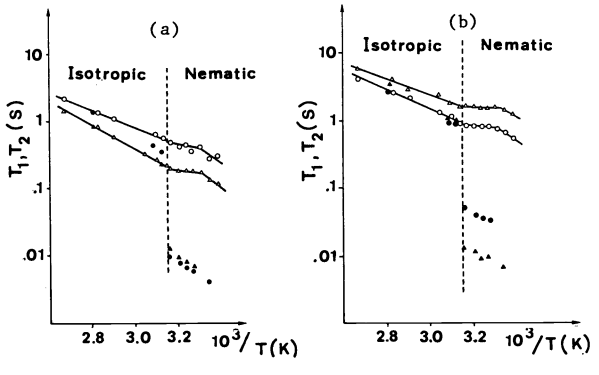


Fig. 9. $T_1$ and $T_2$ relaxation times for various carbons of MBBA, as identified in Fig. 8.
(a) O $C_2$-$T_1$, ● $C_2$-$T_2$, △ $C_3$,$C_7$-$T_1$, ▲ $C_3$,$C_7$-$T_2$ ;
(b) O $C_1$-$T_1$, ● $C_1$-$T_2$, △ $C_{15}$-$T_1$, ▲ $C_{15}$,$T_2$
(After Ref. 37).

TABLE 4 - Rotation constants of MBBA from $^{13}C$ N.M.R.

| T(K) | $D_\perp$ ($cm^2.s^{-1}$) | $D_\parallel$ ($cm^2.s^{-1}$) | $\tau_\perp$ (s) | $\tau_\parallel$ (s) |
|---|---|---|---|---|
| 302 (nematic) | $4.4.10^7$ | $1.1.10^{10}$ | $3.8.10^{-9}$ | $1.5.10^{-11}$ |
| 353 (isotropic) | $2.4.10^8$ | $5.3.10^{10}$ | $6.9.10^{-10}$ | $3.1.10^{-12}$ |

Similar studies have been carried out on TBBA (Table 2) in $S_A$ and $S_C$ phases (Ref. 34) and the resulting curves are shown in Fig. 6. It appears a higher contribution of SD mechanism in the $S_C$ phase than in $S_A$, similarly the rotation of the molecule around the perpendicular axis contributes to the relaxation in $S_C$ whereas it does not in $S_A$. In this latter phase $T_1$ is largely dominated by ODF mechanism.

The isotopic dilution method to separate the inter and intramolecular contributions (mainly SD and ODF mechanisms, respectively)has been applied to $T_1$ and $T_{1\rho}$ on 5 CB (Ref. 35). The results are shown in Fig. 7.

## IV.2 $^{13}C$ N.M.R.

In spite of the various advantages of $^{13}C$ NMR to investigate molecular dynamics, a limited number of such studies have been performed on small molecule liquid crystals.

For MBBA (Table 2), $T_1$ measurements (Ref. 36) as well as $T_1$ and $T_2$ measurements (Ref. 37) have been reported both for isotropic and nematic phases. As an example, proton-spin decoupled spectrum are shown in Fig. 8, the lign assignment is given in the figure. The temperature dependence of $T_1$ and $T_2$ for aromatic and aliphatic carbons is illustrated in Fig. 9.

The main feature is a large drop in $T_2$ when going from isotropic to nematic phase. The change in the temperature dependence of $T_1$ through the I-N transition observed in these curves, has not been found in the previous study (Ref. 36). It appears an increase of $T_1$ values from $C_{15}$ to $C_{18}$ (for this latter, $T_1$ has to be corrected to take into account that it deals with $CH_3$ instead of $CH_2$ for the others) reflecting the increase of mobility along the n-butyl tail. Assuming an anisotropic reorientation motion of the entire molecule, it leads to the diffusion constants and correlation times reported in Table 4; $\tau_\parallel$ is found about $10^{-2}$ times shorter than $\tau_\perp$.

Similar behaviours have been recently obtained for $T_1$ measurements on 5 CB (Table 2) (Ref.38), the same ratio between $\tau_\parallel$ and $\tau_\perp$ is observed, $\tau_\perp$ at 239 K (isotropic phase) is found equal to $1.0.10^{-9}$ s. However, no change in T-dependence of $T_1$ has been found from isotropic to nematic phases.

The different behaviours observed for $T_1$ and $T_2$ show that the high frequency motions are not too much changed by the I-N transition, but the low frequency motions are considerably affected, due to the completely different molecular constraints in the two phases.

## IV.3 Dielectric relaxation

The 4-cyano-4 n-alkyl biphenyl molecules (Table II) constitute the simplest liquid crystal molecules for dielectric relaxation studies for there is only one polar group and besides the dipole moment lies along the molecular long axis. Dielectric measurements with the electric field parallel or perpendicular to the director have been performed on 7 CB (Table 2) in the frequency range $10^5$ Hz-$2.5.10^8$ Hz (Ref. 39).

From quasi-static and high frequency limit permittivities, and by using the value of the order parameter determined from another technique, the correlation-factor g can be deduced; the resulting values are $g_\parallel \simeq 0.30$ and $g_\perp \simeq 0.90$. This latter value indicates that perpendicular to the director there is essentially random orientation of the dipole components, due to the small dipolar component in that direction.

In the isotropic phase, a single relaxation is observed, which corresponds to an isotropic motion (Debye type). In the nematic phase, the parallel arrangement yields a single Debye type relaxation, whereas perpendicular measurements show a broad $\varepsilon''_\perp$ absorption. The T-dependence of the corresponding correlation times, $\tau(DR)$, is presented in Fig. 10.

Let us note that in dielectric relaxation, $\tau_\parallel(DR)$ corresponds to a rotational motion around an axis perpendicular to the director, which fairly means a motion around the molecular short axis, whereas in N.M.R. or E.S.R. such a motion is characterized by a correlation time $\tau_\perp$.

The results shown in Fig. 10 for the isotropic phase are in fair agreement with the average correlation ($\tau_R = (\tau_\parallel . \tau_\perp)^{1/2}$) obtained by $^{13}C$ N.M.R. on 5 CB (Ref. 38). In the nematic phase the ratio $\tau_\parallel(DR)/\tau_\perp(DR)$ ranges from 50 at 293 K to 15 at 308 K, which appears much smaller than what is found from N.M.R.

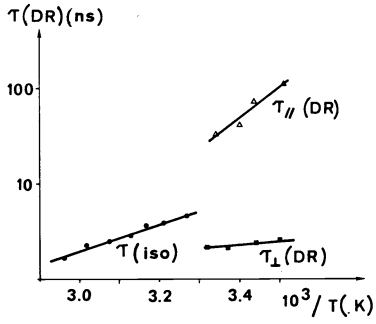


Fig. 10. Dielectric relaxation times vs. $10^3/T$, T in K, in nematic phase ($\tau_{\parallel}$(DR) and $\tau_{\perp}$(DR)) and isotropic phase ($\tau_{iso}$).

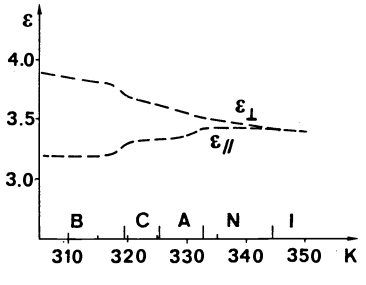


Fig. 11. Temperature dependence of $\varepsilon_{\parallel}$ and $\varepsilon_{\perp}$ for 50-7. (After Ref. 43)

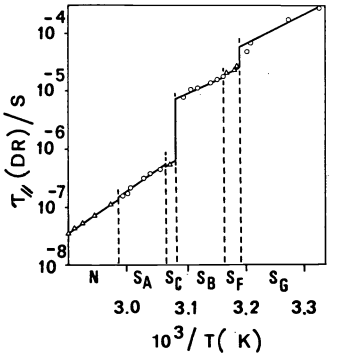


Fig. 12. Dielectric relaxation time, $\tau_{\parallel}$(DR) vs. $10^3/T$ in the various mesophases of 50-6 (After Ref.42)

The treatment of dielectric relaxation in the nematic phase proposed in (Ref. 23) has been successfully applied to these data. Furthermore, the relative intensity of the relaxation processes in the parallel and perpendicular measurements, estimated from the value at the maximum of $\varepsilon''(\parallel)$ and $\varepsilon''(\perp)$, satisfactory agrees with the theoretical prediction. It has to be pointed out that the agreement is not so good with liquid crystal molecules which have internally rotatable polar groups.

Dielectric relaxation studies have been performed on MBBA (Ref. 40 and 41). For a sample oriented in a 1.2 T magnetic field, parallel measurements in the frequency range $10^5$ Hz-$10^7$ Hz (Ref. 40) show a maximum of $\varepsilon''_{\parallel}$, which occurs at $1.1.10^6$ Hz at 295.7 K and agrees with a Debye-type relaxation. On the other hand, no relaxation is observed in this frequency range for perpendicular measurements. In the case of a multi-domain sample, investigations in the frequency range $10^9$ Hz-$10^{10}$ Hz (Ref. 41) show a relaxation in the nematic phase corresponding to correlation times from $2.10^{-10}$ to $1.6.10^{-10}$ sin the temperature range from 295 K to 305 K. Comparison with the corresponding values obtained by $^{13}C$ N.M.R. and reported in Table 4, shows that motions around the molecular short axis have a correlation time almost two orders of magnitude higher in dielectric relaxation, suggesting that in the latter case a cooperative motion could be involved (this interpretation could be supported by the value of the rotation correlation times, $\tau_R$, obtained from $^1H$ N.M.R. and shown in Table 3). For motions around the molecular long axis, a smaller discrepancy is found.

The influence of the nature of the mesophase on the molecular dynamics investigated by dielectric relaxation is quite well illustrated by the studies performed on the series 50-6, 50-7, 50-8 and 60-6 (Ref. 42 - 45).

First of all, the increase in dielectric anisotropy going from $I \rightarrow N \rightarrow S_A \rightarrow S_C \rightarrow S_B$ is shown in Fig. 11 for the 50-7 compound, and the various transitions are easily observed.

The T-dependence of $\tau_{\parallel}$ for 50-6 in the various mesophases is presented in Fig. 12. It is clear that there is no discontinuity at $N \rightarrow S_A$ and $S_A \rightarrow S_C$ transitions, showing that, in spite of the layer structure of $S_A$ and $S_C$ phases, the molecules are still able to rotate around their short axis. A great slowing down of the motion occurs at $S_A \rightarrow S_B$ transitions, corresponding to the in-plane organization of the molecular centers of gravity. However, even if the correlation time is one order of magnitude longer, there is still a possibility for the molecule to rotate around its short axis.

## IV.4 E.S.R.

As an example of E.S.R. investigation of molecular motions in liquid crystal mesophases, we will consider the studies performed on the various phases of 40-6 (Table 2) using nitroxide probes of different sizes and chemical structures. The structures of the considered probes are shown in Table 1, the magnetic axis system ($x_1$, $y_1$, $z_1$) of the nitroxide group being chosen as indicated in Fig. 2. All the studies have been performed on single domain samples.

The transition temperatures for 40-6 are as follow :

$$K \xleftrightarrow{299\ K} S_B \xleftrightarrow{320.3\ K} S_A \xleftrightarrow{327.7\ K} N \xleftrightarrow{249.9\ K} I$$

### *(a) P.D. Tempone probe (ref. 46)*

The magnetic tensor of the probe molecule is not axially symmetric and it appears that the $y_1$ axis is the most oriented along the magnetic field. The T-dependences of the orientational order parameter $S_{y_1z_5}$ and the symmetry term $(S_{x_1y_5} - S_{z_1x_5})$ are shown in Fig. 13 a).

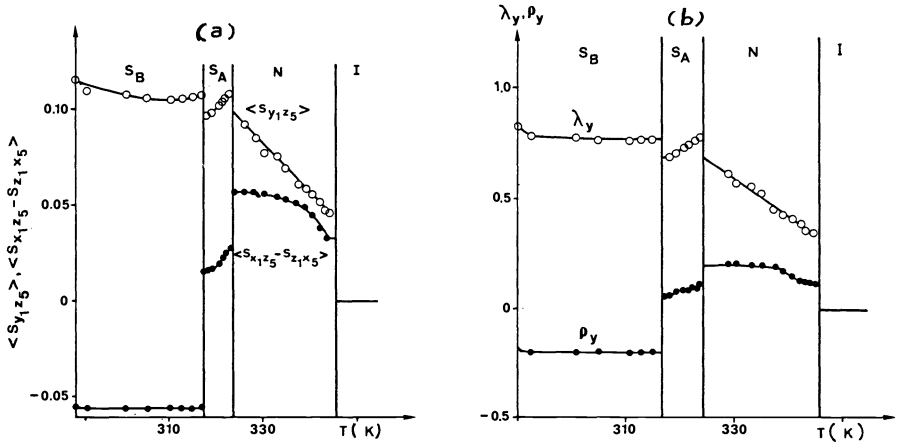


Fig. 13. P.D. Tempone in 40-6 a/ Order parameter $S_{y_1z_5}$ and symmetry term $(S_{x_1z_5}-S_{z_1x_5})$ vs T in K, b/ parameters $\lambda$, $\rho$ of the ordering potential vs. T (After Ref. 46).

Though the spectra can be accounted for considering an axially symmetric ordering potential, a better fit is obtained with a non-axially symmetric potential defined by the two parameters : $\lambda = \gamma_2/kT$ and $\rho = \varepsilon/kT$. These two quantities are represented in Fig. 13 b).

As far as the dynamics is concerned, it has first to be noticed that in the three mesophases the E.S.R. spectra of P.D. Tempone exhibit the typical feature corresponding to motional narrowing. Such a result is not very surprising due to the small size of this probe. The correlation time, $\tau_{\bar{R}}$, is defined by the following relation :

$$\tau_{\bar{R}} = (6\ D_{\bar{R}})^{-1} \text{ with } \bar{D} = (D_{\parallel}\ D_{\perp})^{1/2}$$

where $D_{\parallel}$ and $D_{\perp}$ are the parallel and perpendicular components of the rotational diffusion tensor. In Fig. 14, $\tau_{\bar{R}}$ is plotted vs. $T^{-1}$ for the various mesophases.

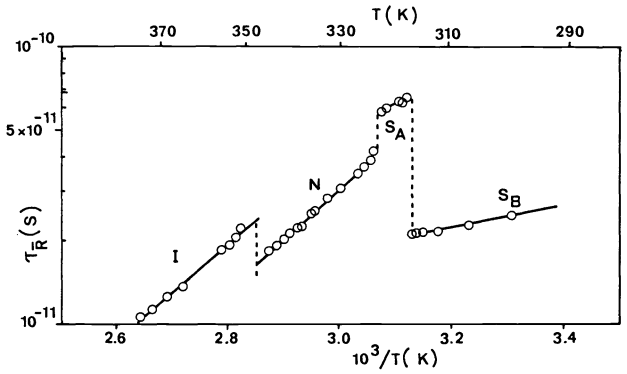


Fig. 14. P.D.Tempone in 40-6. Correlation time, $\tau_{\bar{R}}$, vs.$10^3/T$, (After Ref. 46)

These results have been consistently interpreted considering that the P.D-Tempone is gradually expelled with decreasing temperature from the rigid core region of the 40-6 molecules to the more flexible and less ordered regions of the aliphatic tails when the system successively undergoes the transitions I → N → $S_A$ → $S_B$. The similar apparent activation energies in I and N seem to indicate that the same type of motions occurs in these two phases, what is in agreement with the conclusions reached with the other spectroscopic techniques. The large decrease in $\tau_{\bar{R}}$ from $S_A$ to $S_B$ is surprising, it could correspond to a cavity-like arrangement of P.D-Tempone in the $S_B$ phase, mainly in the aliphatic regions. There would be a partial freezing (or slowing down) of the hydrocarbon end chains at the $S_A$ → $S_B$ transition such that the probe is in a fairly well defined cavity with a reduced frictional restriction to its motion, leading to a large decrease of $\tau_{\bar{R}}$. However, the residual end-chain motions would modulate the structure of the cavity, leading to a SRLS (slowly relaxing local structure) mechanism able to efficiently contribute to the observed line widths.

### *(b) P-Probe (ref. 47)*

In this probe molecule, intramolecular motions may occur, in such away that the magnetic axes of the nitroxyde group may be different from the rotational diffusion axes of the molecule. Furthermore, the mean conformation of the probe molecule may change with temperature and the type of mesophase. Nevertheless, information about these behaviours can be derived from the values and the T-dependence of the order parameters and ordering-potential coefficients. The correlation times $\tau_{\bar{R}}$ and $\tau_{R_\perp}$ ($\tau_{R_\perp} = (6\ D_\perp)^{-1}$) are plotted vs. $T^{-1}$ in Fig. 15.

Contrary to the case of P.D-Tempone it does not seem that any expulsion of P-Probe occurs. In the isotropic phase, the anisotropy parameter $N = D_{\|}/D_\perp$ is equal to 7, what is in agreement with an almost completely extended molecule. The activation energy is the same as for P.D-Tempone, showing that the same molecular motions are involved in both cases, in spite of the different molecular sizes. The I → N transition does not significantly change the activation energy, but there is a slowing down of the motion around the short molecular axis. In the $S_A$ phase, the $\tau_{R_\perp}$ values are still increased, without any change in $\tau_{R_\|}$, this indicates that there is no additional constraint for the motion around the molecular long axis of the probe, but its overall motion is slown down by the increase in frictions forces arising from a better packing in $S_A$ phase. It has to be noticed that in both nematic and $S_A$ phase, the fit with experimental spectra requires a contribution from the SRLS mechanism, the ODF mechanism does not efficiently contribute in this frequency range and its application leads to predictions in the wrong direction. In the $S_B$ phase, which is ordered within the layers, the discontinuity observed for $\tau_{\bar{R}}$ comes from a strong decrease of $\tau_{R_\|}$, the rotational motion around the molecular long axis being constrained by the required motional cooperativity of the surrounding molecules.

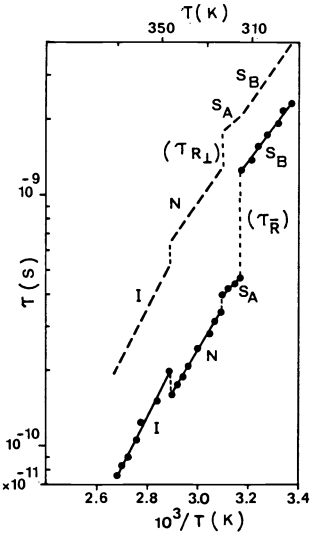


Fig. 15. P-Probe in 40-6. $\tau_{\bar{R}}$ and $\tau_{R_\perp}$ vs. $10^3/T$ (After Ref. (47))

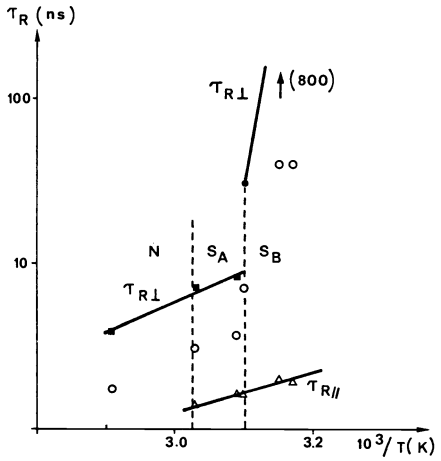


Fig. 16. CSL in 40-6. Correlation times vs. $10^3/T$, for $\tau_{R\|}$, for $\tau_{R\perp}$, for $\tau_{\bar{R}}$

### *(c) CSL Probe (ref. 48)*

In this probe, the nitroxide group cannot undergo any intramolecular motion relatively to the cholestane unit and the intramolecular motions of the rather short aliphatic tail have a small effect on the overall shape of the molecule. Thus, CSL probe can be considered as a quasi-rigid probe with well defined molecular axes and the angles between the molecular long axis and the magnetic axes are known.

The dynamics of the probe correspond to the slow motion regime, though the spectra show three well resolved lines. The T-dependences of $\tau_{\bar{R}}$ and $\tau_{R_\perp}$ are shown Fig. 16. In the nematic phase.

The observed anisotropy parameter (N = 5) is in agreement with the molecular geometry, the correlation times are in the range 2 to $8.10^{-9}$ s, much longer than the ones of the other probes, what is expected due to the large size and high rigidity of the CSL probe. The order parameter is rather high, it reaches 0.77 at 324 K, compared to the values found at the same temperature for P-Probe (0.44) and P.D-Tempone (0.10), and it reaches 0.86 in $S_A$ and $S_B$ phases. These high values reflect that the CSL probe is located very close to the rigid core of the 40-6 molecules, there is no expulsion at all occuring. In $S_A$ and $S_B$ phases, the slowing down of the parallel motion is comparable to that observed with the P-Probe, except that the CSL correlation time, $\tau_{R_\|}$, is one order of magnitude longer. On the other hand, the perpendicular motion of the CSL probe in $S_A$ and $S_B$ phases is considerably hindered, what is not observed with the other probes, the correlation time, $\tau_{R_\perp}$, in the $S_B$ phase is even out of the reach of the E.S.R. technique. In such conditions, the observation of E.S.R. spectra with well resolved lines cannot be explained by considering only the dynamics of the individual probe.

The proposed interpretation is that the CSL probe reorients in a local "cage", the average and instantaneous conformations of which impose restrinctions upon the motion of the probe, so that the overall dynamics is now determined by the combined effect of individual probe modes and collective modes of the surrounding molecules. The SRLS mechanism could be responsible for the dynamic cooperativity.

The above results very well illustrate the problems which arise from the investigation of dynamics of liquid crystals using E.S.R. technique. It is clearly shown that the requirement of an extrinsic probe, the motion of which is observed instead of the dynamics of the liquid crystal molecules, is the main problem. Indeed, the location of the probe is not known and can change with the type of mesophase. To avoid this problem, the synthesis of an analogue of the liquid crystal molecule bearing a nitroxide group is the best way but it implies a specific synthesis. Another difficulty comes from the intramolecular motions of the probe, it can be solved with the CSL probe but it leads to slow motional regime spectra which are more difficult to analyse.

On the other hand, the interest of E.S.R. technique rests in the great sensitivity of the spectra to anisotropic dynamic behaviour and on the very unique possibility to distinguish in the slow motion regime the different motional models (brownian diffusion, jumps...)

## V LOCAL MOLECULAR DYNAMICS IN LIQUID CRYSTAL POLYMERS

Liquid crystal polymers (L.C.P.) may correspond to mesogenic units either in the main-chain or in the side-chains. Of course, the constraints imposed to the dynamics of the mesogenic units by the polymeric nature of the materials are quite different in the two cases.

However, in spite of the partially different behaviours observed for the two types of liquid crystal polymers, there are some characteristic features of polymeric materials compared to small molecule liquid crystals : orientation behaviour and the occurrence of a glass-rubber transition. We will first discuss these topics then we will present some examples of dynamics studies using spectroscopic techniques.

### V.1 Orientation behaviour

Usual bulk polymers in the melt exhibit a flow viscosity which increases as the 3.5 power of their molecular weight. Although the exponent is not yet known for liquid crystal polymers, there is a clear evidence that there is a high molecular weight dependence of the mean flow viscosity. This point is very important when looking at the orientation behaviour of different polymers or samples. Unfortunately, very few molecular weights of such polymers have been determined and the inherent viscosity, $\eta_{inh}$, is frequently the only information available.

In principle, liquid crystal polymers could be oriented and organized in single domain samples by the same procedures as the small molecule liquid crystals, i.e. applying magnetic or electric fields. In practice, the problem arises from the high viscosity of these materials, in particular when main-chain liquid crystal polymers are considered. For a review, see (Ref. 49).

Orientation in a magnetic field at a temperature close to the clearing temperature has been obtained for nematic main chain liquid crystal polymers. For example, a polyester having the repeating unit :

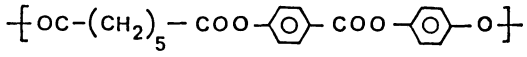

has been oriented parallel to a 0.3 T field (Ref. 50). An order parameter S = 0.64 has been achieved after 24 h for a sample having $\eta_{inh}$ = 0.29 dl/g but a sample with $\eta_{inh}$=0.54 dl/g only reached S = 0.54. Similarly, a copolyester synthesized from terephtalic acid and an equimolar mixture of methylhydroquinone and pyrocatechol has been oriented in field larger than 0.6 T, the orientation time being less than 2 min for a sample of molecular weight 200 000 (Ref. 51). Very large values of S, ranging from 0.72 to 0.88 have been achieved in a 1 T field (Ref. 52) with a polymer having the repeating unit

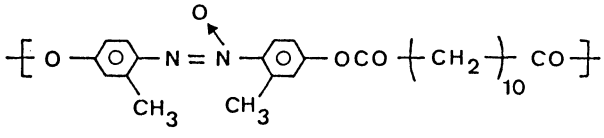

At the opposite, no orientation was obtained in a field as high as 16 T for a polymer with the following structure (Ref. 53).

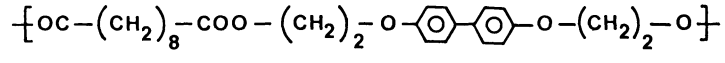

It seems easier to orient the mesomorphic units of side-chain liquid crystal polymers, as it has been done (Ref. 54) with a siloxane polymer of repeating unit :

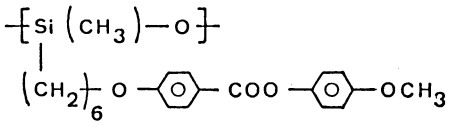

However, it has be noticed that the observed relaxation time is longer for the polymer than for the model compound, in spite of the high flexibility of the siloxane linkage.

Similar behaviours are encountered for orientation in electric field. However, depending on their chemical structure, the mesogenic units can get a positive or negative dielectric anisotropy. In the latter case, it leads to a two-dimensional distribution of the director axes perpendicularly to the applied electric field. Such a situation is found with ester groups and, for example, with the polyester having the repeating unit :

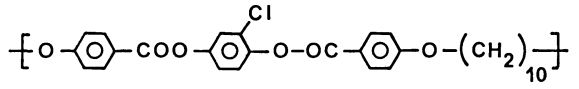

an order parameter S = - 0.5 is achieved in an electric field (E = 50 kV/cm, $\nu$ = 50 KHz) whereas a 7.0 T magnetic field yields S = 1.0 (Ref. 55). Combined effects of perpendicular electric and magnetic fields have been used to orient a ester side-chain liquid crystal polymer with positive diamagnetic and negative dielectric anisotropy (Ref. 56).

## V.2 Glass-transition and secondary transitions

If polymers do not get sufficiently high chemical and stereochemical regularity, they are not able to crystallize and by decreasing the temperature they undergo a transition from a highly viscous liquid to a solid glass, called the glass-transition.

Even for polymers with a high chemical regularity, as for example high density polyethylene, the material never achieves a fully crystalline state and amorphous regions coexist with crystalline regions (semi-crystalline polymers). These amorphous parts of the bulk polymer undergo a glass transition.

The same situation is encountered with liquid crystal polymers. Depending on their chemical structure semi-crystalline states can be obtained or not. However, due to the occurrence for these polymers of nematic and/or smectic phases, the whole material or only the non-crystalline parts of the material will lead to an ordered glassy state which is characterized by a glass transition temperature, Tg (ordered). Such a situation is achieved by slowly cooling down the polymer from the high temperature isotropic state. Of course, if no orientation procedure has been applied, a multi-domain sample would be obtained.

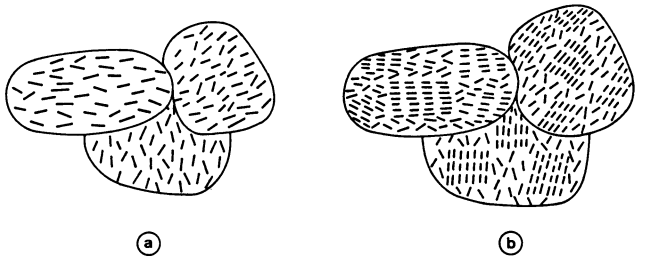


Fig. 17. Schematic representation of a multi-domain sample for a/ a glassy nematic polymer, b/ a semi-crystalline nematic polymer. Only the mesogenic groups are represented.

The resulting structures in the two cases of non-crystalline and semi-crystalline polymers are schematically shown in Fig. 17. If one assumes a nematic phase and one smectic phase occur, the successively observed transitions would be :

- for the non-crystalline case :

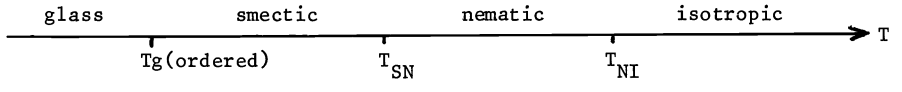


- for the semi-crystalline case :

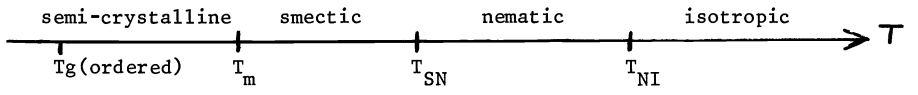

When a very rapid quenching is applied from the isotropic phase, some regions can keep in the rigid solid the disordered structure of the isotropic state, whereas other regions undergo the mesophase-transitions leading to an ordered glassy state. As polymer segments are less constrained in the disordered glass than in the ordered one, samples prepared under such conditions exhibit two glass transition temperatures, this occuring at the lower temperature corresponding to the regions where the isotropic structure has been preserved.

Before considering the effect of the occurrence of a glass transition on the assignment of all the transitions observed by spectroscopic techniques, it is worthwhile recalling that mesophase transitions are thermodynamic transitions, in such a way that the temperatures at which they occur do not depend on the frequency of the technique used for the investigation (calorimetry techniques correspond to frequencies around 1 Hz, spectroscopic techniques cover various frequency ranges as mentioned in III). Concerning the glass transition temperature, an opposite behaviour is observed. Indeed, the glass transition experimentally observed is controlled by the kinetics of the structural changes of the material, thus it has a kinetic nature and the temperature at which it is observed depends on the frequency of the investigating technique. Typically, the glass transition temperature is upwards shifted by 5°C to 10°C when the measurement frequency is increased by a factor 10. A commonly used relation to quantitatively account for the glass transition temperature shift is the so-called W.L.F. equation (Ref. 57) :

$$\mathrm{Log}(f_2/f_1) = -A[\,Tg(f_1) - Tg(f_2)]/[B + (Tg(f_1) - Tg(f_2))]$$

where $Tg(f_1)$, $Tg(f_2)$ are the glass transition temperatures observed at the frequencies $f_1$ and $f_2$ respectively, and A, B are constants which slightly depend on the polymer but can be assumed as universal in a first approximation. This relation can be derived from the free volume theory, it describes a non-Arrhenian behaviour of the molecular phenomena responsible for the glass transition.

In addition to the glass transition, most of polymers exhibit in the solid state secondary transitions (β, γ, etc.) which correspond to motions of groups in side-chain or main chain, as for example the β-transition observed in polyacrylates (R =H) or methacrylates (R = $CH_3$) :

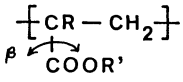


which is assigned to a rotational motion of the ester group around its linkage to the main chain. These secondary transitions are characterized by a frequency dependence which corresponds to an Arrhenian activated process.

The various transitions undergone by a bulk polymer are usually represented in a "relaxation map", as typically shown in Fig. 18 a/, where log f vs. 1/T is plotted for each transition.

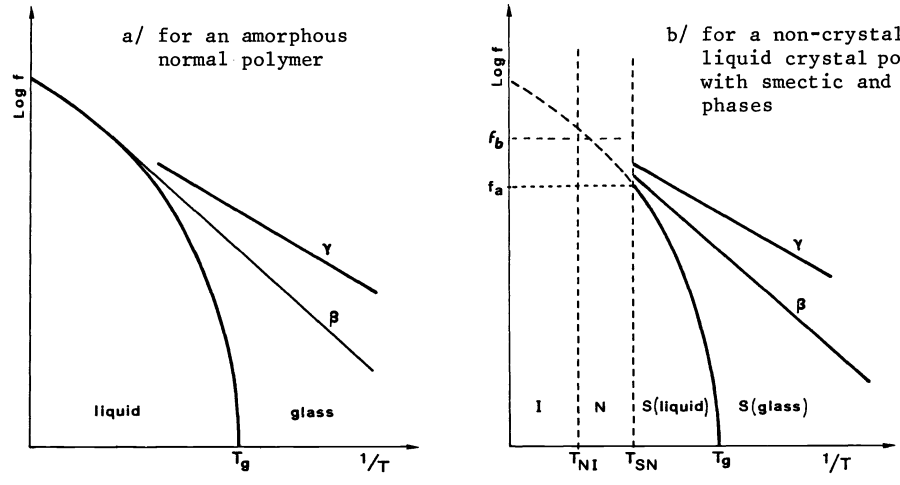


Fig. 18 . Schematic relaxation maps

At high temperature and high frequencies, glass transition and β-transition could merge together.

For a liquid crystal polymer, in addition to the secondary and glass transition, mesophase transitions occur which correspond to temperatures independent of frequencies, as schemed in Fig. 18 b) for a non-crystalline system where a nematic phase and a smectic phase exist. Thus, for low frequency measurements, by increasing temperature the following transitions successi-

vely appear : $\gamma$, $\beta$, glass transition, S - N and N - I. At higher frequencies, but lower than the frequency, $f_a$, where $Tg(f_a)$ is equal to $T_{SN}$, the same behaviour is observed and, in particular, the glass transition associated with the ordered glassy state (in Fig. 18 it would be a smectic glassy state) can be detected. At frequencies higher than $f_a$ (for example $f_b$ in Fig. 18 b) molecular motions in the isotropic, nematic, smectic liquid phases or solid state can be investigated, but the high frequency glass transition of the smectic glassy state will no more exist because the smectic-nematic transition will change the original smectic structural arrangement of the polymer segments.

These features are very important for assigning the various transitions observed using spectroscopy motions. In particular, a transition occuring at high frequency in a temperature range where the glass transition is observed by calorimetry experiments does not correspond to the glass transition process but to secondary relaxations ($\beta$, $\gamma$, etc.).

Finally, it is clear from the above considerations that to study with a spectroscopic technique operating at a frequency F, molecular processes involved in the glass transition of the ordered glass it is necessary that the mesophase encountered in the glassy state remains till a temperature higher than Tg(F). Typically, to perform such a study at $10^5$ Hz, it is required that the polymer does not undergo any mesophase transition at a temperature lower than Tg(calorimetry) + 50°C (at $10^8$ Hz, it would become Tg(calorimetry) + 80°C).

## V.3. Spectroscopic studies of local dynamics in liquid crystal polymers

Very few studies have already been published on liquid crystal polymers using the spectroscopic techniques considered in this paper. In addition, except for the study in (Ref. 59) only one technique has been used in each case : E.S.R. in (Ref. 56 and 60) dielectric relaxation in (Ref. 61 - 67), $^{13}C$ N.M.R. in (Ref. 68).

### *(a) Side-chain liquid crystal polymers*

Dielectric relaxation experiments have been performed on various side-chain liquid crystal polymers. Thus, investigations of dynamic behaviour in mesophase and isotropic phase have been carried (Ref. 61 - 64) out on polymers with the following repeat units :

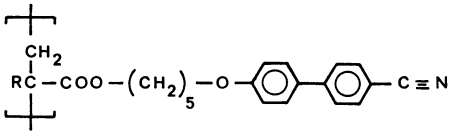


samples with R = H, $CH_3$ will be later referred to as PACB and PMACB respectively. The phase transitions determined from calorimetry experiments are :

$$\text{PACB} = \text{g} \overset{323\ \text{K}}{\longleftrightarrow} \text{N} \overset{360\ \text{K}}{\longleftrightarrow} \text{I}$$

$$\text{PMACB} = \text{g} \overset{333\ \text{K}}{\longleftrightarrow} \text{S} \overset{397\ \text{K}}{\longleftrightarrow} \text{I}$$

Measurements on multi-domain samples yield temperature dependences of the frequency at the maximum of $\varepsilon''$ shown in Fig. 19. For PACB a small increase in frequency occurs at the N - I transition whereas it is thrice larger at the S - I transition of PMACB. A decrease in the apparent activation energy is observed in both cases between the mesophase and the isotropic state. For PACB, a partially oriented sample was obtained by applying an electric field and relaxation measurements were performed with the electric field parallel or perpendicular to the director. In addition to the low frequency absorption, in the two cases a high frequency relaxation exists. For example, at 321.9 K, the frequency values are : $F_{\parallel 1}$ = 1.7 Hz, $F_{\parallel 2} \simeq$ 200 Hz and $F_{\perp 1}$ = 2.5 Hz, $F_{\perp 2} \simeq$ 200 Hz but the relaxation amplitude is twice smaller for perpendicular than for parallel arrangement. From the data reported in Table 5 it is clear

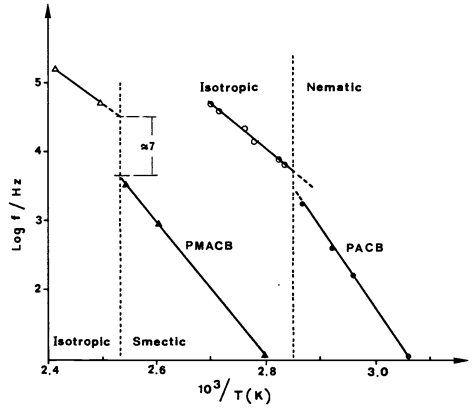


Fig. 19. Log f/Hz vs $10^3/T$ for PACB and PMACB in mesomorphic and isotropic states

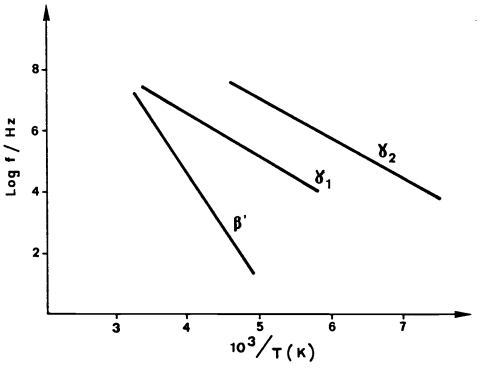


Fig. 20. Typical dielectric relaxations in the solid state

that the reorientation of the mesogenic group around the main chain, corresponding to the parallel relaxation, is about hundred times slower than the rotational motion of the side chain around its long axis. The relaxation frequency measured on a multi-domain sample mainly reflects the reorientation motion of the mesogenic group. It is interesting to compare these results with the correlation times observed on the small molecule liquid crystal 7 CB (Table 2) and shown in Fig. 10. It appears that the chain backbone considerably slows down the motions of the cyanobiphenyl group, as well for reorientation motions around an axis perpendicular to the biphenyl axis as for rotational motions around the molecular long axis.

A series of side-chain polymers has been recently studied by dielectric relaxation in the frequency range $10^{2}$ - $10^{7}$ Hz for both solid and liquid states (Ref. 66). The general formula of the repeating unit is :

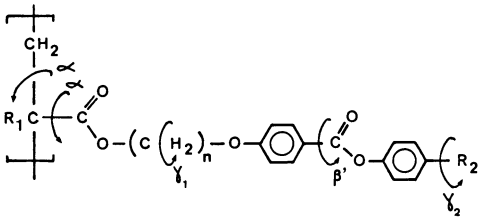

Table 5 - Relaxation frequencies for partially oriented ($F_{\parallel 1}$, $F_{\perp 2}$) and isotropic multi-domain samples

| T(K) | 321.9 | 331 | 342.2 | 353.7 |
|---|---|---|---|---|
| $F_{\parallel 1}$ [Hz] | 1.7 | 28 | 290 | 2100 |
| $F_{\perp 2}$ [Hz] | 200 | 2000 | 20 000 | ≃150 000 |
| F [Hz] | 7 | 110 | 800 | 5000 |

where $R_1$ = H or $CH_3$, n = 2 or 6 and $R_2$ = CN, $OCH_3$, $O(CH_2)_3CH_3$. The samples were not oriented. Depending on the chemical structure, several transitions have been observed in the solid state, they are schematically represented in the relaxation map shown in Fig. 20. The β' transition is observed at the same position independly of the nature of $R_1$ and $R_2$ and of the length of the spacer; its apparent activation energy is 50 ± kJ.mol$^{-1}$. Such a behaviour suggests to assign this transition to an internal motion of the mesogenic group. Indeed, compared to the β relaxations of polymethacrylate (PMAD) and polyacrylate derivatives (PAD) which are attributed to a rotational motion of the ester group relatively to the chain backbone, this β'relaxation appears very different for several reasons (Ref. 69) : 1/ at a given frequency, the β transition of PAD occurs at much lower temperatures than that of PMAD (the temperature shift is around 120 K) 2/ the apparent activation energy of the β-transition is about 84 kJ.mol$^{-1}$ for PMAD and 42 kJ.mol$^{-1}$ for PAD. The fact that the relaxation associated to the rotation of the ester group next to the chain backbone is not found in these side-chain liquid crystal polymers could originate from the large decrease in the amplitude of the β relaxation observed in PMAD when the size of the substituent is increased. Concerning the $\gamma_1$ transition it is only observed for the longer spacer ($n_1$ = 6) and does not depend on $R_1$ and $R_2$; its apparent activation energy is 35 ± 10 kJ.mol$^{-1}$. It has been assigned to motions initiated by the $(CH_2)_6$ sequence of the side chain and becoming dielectrically active because of the coupling to the adjacent dipole moments. The $\gamma_2$ transition only occurs in polymers with $R_2$ = O $C_4H_9$, consequently it corresponds to a motion localized in this sequence. The dielectric relaxations (noted α) and shown in Fig. 21 for a few compounds can be very well extrapolated to the corresponding calorimetric glass transition temperatures, furthermore some of them exhibit a non-Arrhenian behaviour and the frequency greatly depends on temperature (the mean slope yields typical apparent activation energy in the range 150 - 350 kJ.mol$^{-1}$). The main chain motions involved in the glass transition is observed in dielectric relaxation for they cause a reorientation of the adjacent ester dipole. Finally,

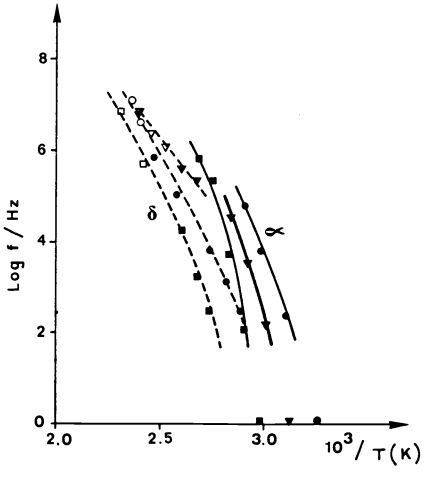


Fig. 21. Dielectric relaxations in the liquid state.
Log f/Hz vs. $10^3$T. α relaxation corresponds to solid lines and δ relaxation to dotted lines.
Polymer samples : □ , $R_1$ = H, n = 2, $R_2$ = $OCH_3$; ○ , $R_1$ = H, n = 6, $R_2$ = CN; ▽ , $R_1$ = $CH_3$, n = 6, $R_2$ = $OCH_3$;
(filled symbols : nematic or smectic phase; open symbols : isotropic phase) (After Ref. 66)

at higher temperature, for polyacrylate compounds ($R_1$ = H), another dielectric relaxation (noted δ) is observed both in mesomorphic and isotropic liquid states (Fig. 21). Its amplitude is much higher for CN end group than for $OCH_3$ or $OC_4H_9$, indicating that it is related to a motion implying some reorientation of the mesogenic unit. Furthermore, comparison with the results above reported in Table 5 shows that the δ relaxation frequency lies in the same range, so the same molecular mechanism could be responsible for it. It has to be noticed that the δ relaxation, first is very weak for the polyacrylates with a short spacer and, secondly it is not found for polymethacrylates where only one transition, related to the glass transition, is observed except in the case of n = 6 and $R_2 = OC_4H_9$ where a δ transition occurs. These last remarks could support an interpretation of the δ relaxation as a reorientation motion of the mesogenic group perpendicularly to the local chain backbone axis which would be facilitated by a more flexible chain backbone (i.e. $R_1$ = H instead of $R_1 = CH_3$) or a longer spacer. Such a reorientation motion would be similar to the one observed in small molecule liquid crystals, except that in the case of side-chain liquid crystal polymers it is considerably slown down. It does not seem that the frequency of this motion undergoes any discontinuity at the mesophase transitions neither at the clearing temperature.

In the field of side-chain liquid crystal polymers, an E.S.R. study has been performed (Ref.56 and 60) on compounds with the following structures :

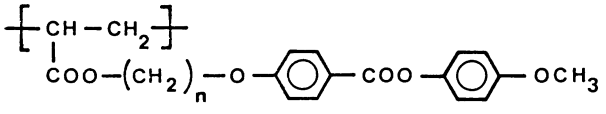

with two spacer lengths (n = 2 for P 2 and n = 6 for P 6). Samples had molecular weights in the range 4500 - 21 000 for P 2 and 2500 - 14 000 for P 6. The corresponding phase transitions are :

P 2a ($\bar{M}_n$ = 21 000) g $\overset{334\ K}{\longleftrightarrow}$ N $\overset{388\ K}{\longleftrightarrow}$ I

P 6a ($\bar{M}_n$ = 14 000) g $\overset{302\ K}{\longleftrightarrow}$ $S_A$ $\overset{367\ K}{\longleftrightarrow}$ N $\overset{393\ K}{\longleftrightarrow}$ I

Oriented samples were obtained by combined effects of perpendicular magnetic and electric fields. The chosen nitroxide group was the CSL probe (see Table 2) which is rigid and appears to be located exclusively in the side-chain region, as indicated by the measured order parameter. For both polymers the anisotropy coefficients ($N = \tau_{R\perp}/\tau_{R\parallel}$, where $\tau_{R\parallel}$ and $\tau_{R\perp}$ are the correlation times for motions around the molecular long and short axes, respectively) are the same and equal to 7 in the isotropic phase and 10 in the nematic and smectic phases. No significant effect of the molecular weight has been observed and the T-dependence of $\tau_{R\parallel}$ is plotted versus 1/T in Fig. 22. It first appears that increasing the spacer length from n = 2 to n = 6, yields a decrease of correlation times by about one order of magnitude for the isotropic and nematic phases, whereas there is no effect in the glassy state as we could expect. Only the smectic-nematic transition leads to an abrupt change in correlation times. The break in slope observed at a temperature around the calorimetric glass transition has not to be assigned to the glass transition phenomena, as it has been proposed in (Ref. 56) for the high frequency E.S.R. measurements should yield a much higher glass transition temperature, as above developed. More likely, such breaks reflect the occurrence of a local motion in

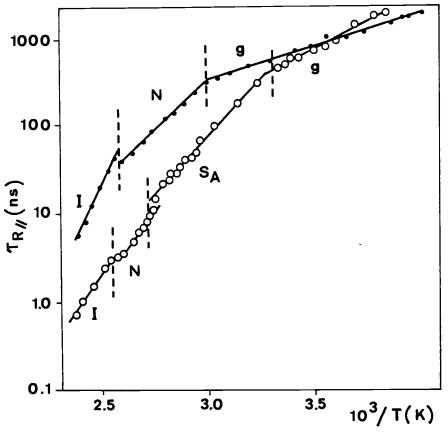


Fig. 22. $\tau_{R\parallel}$ vs. $10^3$/T for CSL in P2a (full circles) and P6a (open circles). (After Ref. 56)

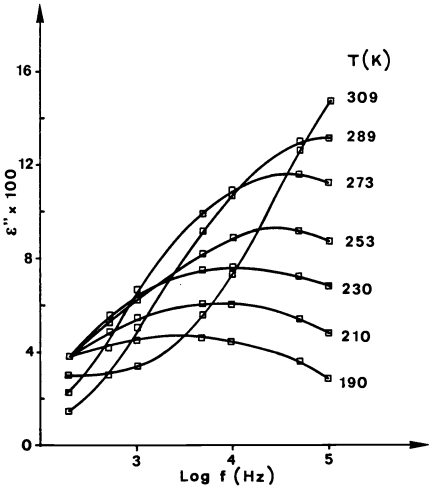


Fig. 23. The dielectric loss factor ε" as a function of frequency for given temperatures. (After Ref. 59)

the E.S.R. frequency range which could be related to a β-process. In absence of complementary experiments (dynamic mechanical studies, dielectric relaxation, N.M.R.) it is not possible to assign this local motion.

### *(b) Main-chain liquid crystal polymers*

In addition to E.S.R. investigation (Ref. 58), dielectric and $^{13}C$ N.M.R. measurements (Ref. 59) have been performed on a main chain liquid crystal polymer with the following repeating unit:

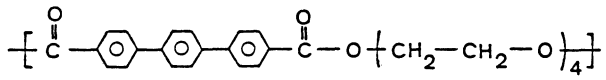

In the solid state, the investigated samples contain a few isolated regions of disordered (amorphous isotropic) material, dispersed in a semi-crystalline continuum. The various calorimetric transitions are :

$$g_{(1)} \overset{233\ K}{\longleftrightarrow} g_{(2)} \overset{293\ K}{\longleftrightarrow} \underline{K} \overset{393\ K}{\longleftrightarrow} S_C \overset{523\ K}{\longleftrightarrow} I$$

It has not been possible to orient the samples in 1 T magnetic field and all the experiments deal with mesomorphic multi-domain samples.

Dielectric relaxation measurements have been performed in the low temperature range and ε'' vs Log f(Hz) is plotted in Fig. 23. At 193 K a relaxation process occurs with a small amplitude indicating a limited freedom of dipoles. The absorption peak, with a maximum around $5 \cdot 10^3$ Hz, is very broad, which suggests that there is a wide variety of local environments for the dipoles and that environment places great constraints on the motion. A given dipole group can move only in cooperation with that environment, this being overall a slow process. As the temperature is increased, the whole system cooperatively moves faster, narrowing the overall loss peak. As a consequence, at high enough temperatures a reference group moves in an average environment. From the shift of the maximum of ε'' with temperature, an apparent activation energy of 16 $KJ.mol^{-1}$ is deduced. It is worthnoting that in the same frequency-temperature range a similar relaxation is observed in poly aliphatic ethers which has been assigned to a local twisting motion.

The motions involved in this relaxation process have been analysed by $^{13}C$ solid state high resolution N.M.R. at 298 K. It appears that at the frequency involved in the considered relaxation methods, i.e. $10^5$ Hz, the carbonyl group and the nearest $CH_2$ group have a rigid behaviour whereas the next-nearest $CH_2$ group undergoes oscillations on the valence cone of approximately 20° about one equilibrium conformation. The following $CH_2$ group performs oscillations of large amplitude or more likely jumps between two equilibrium conformations, as for example a three bond motion corresponding to a $g^+ \leftrightarrow g^-$ conformational jump (Ref. 70).

Several nitroxide probes of different sizes have been studied and it has been shown that in the very slow-motional regime ($\tau \geqslant 10^{-8}$ s) small probes as Tempol (see Table 2) undergo jump diffusion motions whereas large probes have a brownian rotational diffusion. The most characteristic E.S.R. spectra obtained for Tempol in the temperature range 113 K - 423 K are shown in Fig. 24. At 203 K the separation of the outer hyperfine extrema slightly decreases with increasing temperature, indicating the onset of slow motion of the spin probe due to local main chain motions. These motions are the same as those observed by dielectric and $^{13}C$ rela-

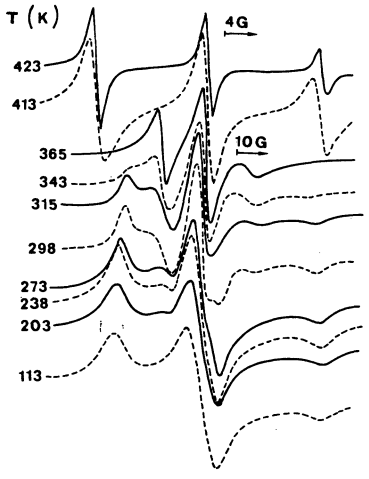


Fig. 24. E.S.R. spectra of Tempol probe for given temperatures

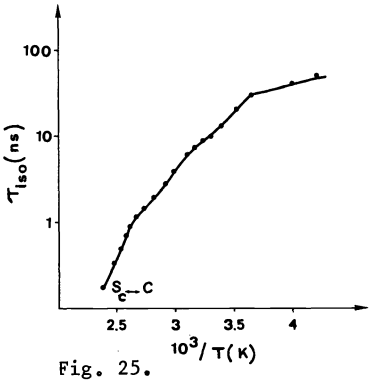


Fig. 25. Isotropic rotational correlation time $\tau_{iso}$, vs. $10^3$T for tempol probe

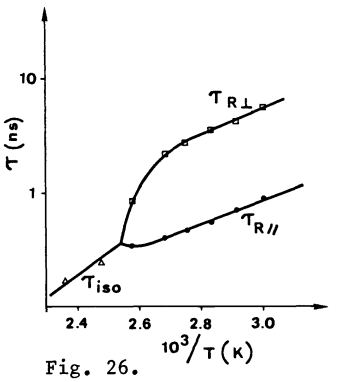


Fig. 26. Correlation times, $\tau_{R\parallel}$, $\tau_{R\perp}$ and $\tau_{iso}$ vs. $10^3/T$ for Tempol probe

xation and above assigned to conformational jumps of the central part bonds of the aliphatic ether sequences of the liquid crystal polymer chain. In order to get information on the correlation times of motions performed by the nitroxide probes over the whole investigated temperature range, E.S.R. spectra have been treated assuming an isotropic reorientation. Resulting isotropic correlation times, $\tau_{iso}$, for Tempol are plotted vs 1/T in Fig. 25. It is clearly seen that $\tau_{iso}$ does not fit an Arrhenius type expression over the whole temperature range. From 203 K till 273 K the Tempol probe reflects the conformational jumps of the aliphatic ether sequences, proving that the probe molecules would be preferentially localized in the interlayer regions of the $S_C$ phase. A change in the slope of the Arrhenius plot of $\tau_{iso}$ is observed around 273 K, corresponding to an increase in the probe mobility. Furthermore complex E.S.R. spectra are observed (Fig. 23) which can be resolved into a mobile component and a solid state component. The same behaviour is found for a similar polyester with 10 ethylene oxide units instead of 4 in the considered polymer. Besides, heat capacity measurements and dynamic mechanical experiments performed on samples submitted to different cooling cycles allow to assign the transition observed with these techniques around 233 K and corresponding in E.S.R. to the appearance of a mobile component at 273 K, to a few isolated disordered regions of the material. As the same E.S.R. behaviour is found in nitroxide doped-PEO spectra (Ref. 71), this suggests that this transition is due to the diffusional segmental motion of the flexible aliphatic ether sequences of the polymer chain; it could correspond to the glass transition of the disordered glassy state. At higher temperature, a marked increase in heat capacity is evidenced between 293 K and 323 K which is associated with the glass transition of the $S_C$ glassy regions of the material. In this temperature range, the solid state component of the Tempol E.S.R. spectra gradually shifts towards the mobile component and finally both components coalesce around 318 K. At still higher temperature, the slope of the Arrhenius plot of $\tau_{iso}$ is changed, however the E.S.R. spectra show the characteristic features of spin probe undergoing anisotropic rotational reorientation. The corresponding anisotropy parameter of Tempol, $N=\tau_{R\perp}/\tau_{R\parallel}$, is about 7, whereas it should be 1.35 from the molecular geometry. The T-dependences of $\tau_{R\perp}$ and $\tau_{R\parallel}$ are plotted in Fig. 26. About 20 K below the crystal-$S_C$ transition (393 K), a "premelting" effect occurs, yielding a decrease in the degree of anisotropy with increasing temperature. Finally at the crystal-$S_C$ transition, the rotation of Tempol is temporarily isotropic. A further increase in temperature results in a marked change of the E.S.R. spectrum shape : above 400 K the low-field line is sharper than the center field line. This unusual behaviour can be interpreted in considering that the orientation of the anisotropic diffusion axis with respect to the nitroxide radical magnetic axes changes upon passing through the crystal-$S_C$ transition, this means that the fastest rotational motion of the Tempol probe does not occur around the same axis, may be due to the lower constraints in the $S_C$ phase compared to the crystal state. Finally, it is worthnoting that $^{13}C$ solid state N.M.R. studies (Ref. 68) have shown that at the crystal-$S_C$ transition, the width of the aromatic carbon line strongly decreases and the associated chemical shift anisotropy change indicates a rotation of the phenyl rings around the $C_1 - C_4$ axis in the mesophasic state. However, such a motion does not alter the mean orientation of the mesogenic groups.

In spite of the partial experimental investigations performed on the dynamic behaviour of this main chain polymer , this example clearly illustrates the better knowledge on a molecular level which arises from a combination of different spectroscopic techniques.

## VI CONCLUSION

In this paper we have presented dynamic spectroscopic studies performed on liquid crystal systems of either small molecules or polymer chains; in this latter case both side-chain and main-chain liquid crystal polymers have been considered. From the obtained results it clearly appears that spectroscopic techniques such as $^1H$, $^{13}C$ N.M.R., E.S.R. and dielectric relaxation can provide information on molecular motions occurring in these ordered phases. However, it is worthnoting that a deep analysis of the results on a molecular scale requires oriented samples. In spite of the experimental difficulty to get such an orientation of the material, the benefit which is then obtained fully justifies the effort. Furthermore, combined experiments using different techniques are the only way to achieve a molecular description of the dynamics of the considered system. Though $^{13}C$ N.M.R. appears to be the most attractive method, yielding information on the dynamic behaviour of the different groups in the molecule, complementary data obtained from other techniques are required to analyse the $^{13}C$ relaxation measurements in taking into account the different types of rotational motions which can participate to the observed relaxation (intramolecular motions, diffusional motions, orientation director fluctuations or slow relaxations of local structures).

In the field of liquid crystal polymers, though only a few partial investigations have been already performed, they appear very promising and a deeper insight on the dynamics of these materials should be reached in a near future.

## ACKNOWLEDGMENT

The author wishes to thank Dr. F. Lauprêtre and specially Dr. C. Noël for very valuable discussions on the presented topic.

## REFERENCES


1. D. Demus, L. Richter, Textures of Liquid Crystals, Verlag Chemie, Weinheim (1978)
2. G.W. Gray, J.W.G. Goodby, Smectic Liquid Crystals, Leonard Hill, Glasgow (1984)
3. W. Maier, A. Saupe, Z. Naturforsch. A, 13, 564 (1958); 14, 882 (1959); 15, 287 (1960)
4. J. Cognard, in Molecular Crystals and Liquid Crystals, Suppl. 1, p. 1, Gordon and Breach, (1982)
5. H. Kelker, R. Hatz, Handbook of Liquid Crystals, Verlag Chemie, Weinheim (1980)
6. H.J. Deuling, in Solid State Physics, Suppl. 14, Liquid Crystals, L. Liebert, ed., p. 77, Academic Press, New-York (1978)
7. E. Dubois-Violette, G. Durand, E. Guyon, P. Manneville, P. Pieranski, in Solid State Physics, Suppl. 14, Liquid Crystals, L. Liebert, ed., p. 147, Academic Press, New-York (1978)
8. W.R. Krigbaum, in Polymer Liquid Crystals, A.C. Ferri, W.R. Krigbaum, R.B. Meyer, ed., p. 275, Academic Press, New-York (1982)
9. A. Abragam, The Principles of Nuclear Magnetism, Oxford University Press (1961)
10. F.W. Wehrli, T. Wirthlin, Interpretation of Carbon-13 N.M.R. spectra, Heyden, London (1976)
11. T.C. Farrar, E.D. Becker, Pulse and Fourier Transform N.M.R., Academic Press, New-York (1971)
12. M. Mehring, High Resolution N.M.R. Spectroscopy in Solids, N.M.R. Vol. 11, Springer Verlag, Berlin (1976)
13. A. Pines, J.J. Chang, Phys. Rev. A, 10, 946 (1974)
14. L.J. Berliner, ed., Spin Labeling, Academic Press, New-York (1976)
15. N.M. Atherton, Electron Spin Resonance. Theory, Applications, Wiley, New-York (1973)
16. W. Gordy, Theory and Applications of Electron Spin Resonance, Wiley, New-York (1980)
17. L. Monnerie, in Static and Dynamic Properties of the Polymeric Solid State, R.A. Petrick, R.W. Richards, ed., p. 271, D. Reidel, Dordrecht (1982)
18. N. Hill, W.E. Vaughan, A.H. Price, M. Davies, Dielectric Properties and Molecular Behaviour, Van Nostrand, New-York (1969)
19. N.G. Mc Crum, B.E. Read, G. Williams, Anelastic and Dielectric Effects in Polymeric Solids, Wiley, London (1967)
20. P. Hedvig, Dielectric Spectroscopy of Polymers, Adam Hilger, Bristol (1977)
21. G. Williams, Adv. Polymer Sci., 33, 59 (1979)
22. W.H. de Jeu, The Dielectry Permittivity of Liquid Crystals, in Solid State Physics, Suppl. 14, Liquid Crystals, L. Liebert, ed., p. 109, Academic Press, New-York (1978)
23. G. Meier, A. Saupe, Mol. Cryst. Liq. Cryst., 1, 515 (1966)
24. P. Bordewijk, Physica, 75, 146 (1974)
25. W. Williams, M. Cook, P.J. Hains, J. Chem. Soc. Farad. Trans II, 68, 1045 (1972)
26. J.H. Freed, J. Chem. Phys., 66, 4183 (1977)
27. P.L. Nordio, U. Segre, in The Molecular Physics of Liquid Crystals, G.R. Luckhurst, G.W. Gray, ed., p. 411 and p. 427, Academic Press, London (1979)
28. P.L. Nordio, U. Segre, Mol. Phys., 25, 129 (1973)
29. C.F. Polnaszek, G.U. Bruno, J.H. Freed, J. Chem. Phys., 58, 3185 (1973)
30. C.F. Polnaszek, J.H. Freed, J. Phys. Chem., 79, 2283 (1975)
31. P.G. de Gennes, The Physics of Liquid Crystals, Clarendon Press, London (1974)
32. P. Pincus, Solid State Comm., 7, 415 (1969)
33. V. Graf, F. Noack, M. Stohrer, Z. Naturforsch, A, 32, 61 (1977)
34. R. Blinc, M. Vilfan, M. Luzar, J. Seliger, V. Zagar, J. Chem. Phys., 68, 303 (1978)
35. J.S. Lewis, E. Tomchuk, E. Bock, Mol. Cryst. Liq. Cryst., 97, 387 (1983)
36. M. Hutton, E. Bock, E. Tomchuk, R.Y. Dong, J. Chem. Phys., 68, 940 (1978)
37. S. Ochiai, K. Iimura, M. Takeda, M. Ohuchi, K. Matsushita, Mol. Cryst. Liq. Cryst., 78 227 (1981)
38. J.S. Lewis, E. Tomchuk, H.M. Hutton, E. Bock, J. Chem. Phys., 78, 632 (1983)
39. M. Davies, R. Moutran, A.H. Price, M.S. Beevers, G. Williams, J. Chem. Soc. Farad. Trans. II, 72, 1447 (1976)
40. F. Rondelez, A. Mirrea-Roussel, Mol. Cryst. Liq. Cryst., 28, 173 (1974)
41. J.K. Moscicki, X.P. Nguyen, S. Urban, S. Wrobel, M. Rachwalsi, J.A. Janik, Mol. Cryst. Liq. Cryst., 40, 177 (1977)
42. H. Kresse, Ch. Selbmann, D. Demus, A. Buka, L. Bata, Cryst. Res. Technol., 16, 1439 (1981)
43. L. Benguigui, J. Phys., 41, 341 (1980)
44. L. Benguigui, Phys. Rev. A, 28, 1852 (1983)
45. L. Benguigui, Phys. Rev. A, 29, 2968 (1984)
46. W.J. Lin, J.H. Freed, J. Phys. Chem. 83, 379 (1979)
47. E. Meirovitch, D. Igner, E. Igner, G. Moro, J.H. Freed, J. Chem. Phys., 77, 3915 (1982)
48. E. Meirovich, J.H. Freed, J. Phys. Chem., 84, 2459 (1980)
49. W.R. Krigbaum, in Polymer Liquid Crystals, A. Ciferri, W.R. Krigbaum, R.B. Meyer, ed., p. 275, Academic Press, New-York (1982)
50. L. Liebert, L. Strzelecki, D. Van Duyen, A.M. Levelut, Eur. Polym. J.,17, 71 (1981)
51. C. Noël, L. Monnerie, M.F. Achard, F. Hardouin, G. Sigaud, M. Gasparoux, Polymer, 22, 578 (1981)
52. F. Volino, A.F. Martins, R.B. Blumstein, A. Blumstein, C.R. Heb. Acad. Sci., Ser. II, 292, 829 (1981)
53. G. Maret, A. Blumstein, S. Vilasagar, Polym. Prepr., Am. Chem. Soc., Div. Polym. Chem., 22, 246 (1981)
54. C. Casagrande, M. Veyssié, C. Weill, H. Finkelmann, Mol. Cryst. Liq. Cryst. (Lett.), 92 49 (1983)
55. K. Müller, K-H. Wassmer, R.W. Lenz, G. Kothe, J. Polym. Sci. Polym. Lett. Ed., 21, 785 (1983)
56. K-H. Wassmer, E. Ohmes, M. Portugall, H. Ringsdorf, G. Kothe, J. Am. Chem. Soc., 107, 1511 (1985)
57. J.D. Ferry, Viscoelastic Properties of Polymers, 3 rd ed., Wiley, New-York (1980)
58. P. Meurisse, C. Friedrich, M. Dvolaitzky, F. Lauprêtre, C. Noël, L. Monnerie, Macromolecules, 17, 72 (1984)
59. F. Lauprêtre, C. Noël, W.N. Jenkins, G. Williams, Faraday Discussion n°79 : Polymer Liquid Crystals (1985)
60. H-K. Wassmer, E. Ohmes, G. Kothe, M. Portugall, H. Ringsdorf, Makromol. Chem. Rapid Comm. 3, 281 (1982)
61. H. Kresse, R.V. Talrose, Makromol. Chem., Rapid Comm., 2, 369 (1981)
62. H. Kresse, S. Kostromin, V.P. Shibaev, Makromol. Chem., Rapid Comm., 3, 509 (1982)
63. H. Kresse, V.P. Shibaev, Z. Phys. Chemie, Leipzig, 264, 161 (1983)
64. H. Kresse, V.P. Shibaev, Makromol. Chem., Rapid. Comm., 5, 63 (1984)
65. R. Zentel, G.R. Strobl, H. Ringsdorf, in Recent Advances in Liquid Crystal Polymers, L.L. Chapoy, ed., p. 261, Elsevier, London (1985)
66. R. Zentel, G.R. Strobl, H. Ringsdorf, Macromolecules, in press
67. W. Haase, H. Pranoto, in Polymeric Liquid Crystals, A. Blumstein, ed., p. 313, Plenum Press, New-York (1985)
68. P. Sergot, F. Lauprêtre, C. Louis, J. Virlet, Polymer, 22, 1150 (1981)
69. N.G. Mc Crum, B.E. Read, G. Williams, Anelastic and Dielectric Effects in Polymeric Solids, Wiley, New-York (1967)
70. F. Gény, L. Monnerie, J. Polymer Sci., Polym. Phys. Ed., 17, 131 and 147 (1979)
71. M.C. Lang, C. Noël, A.P. Legrand, J. Polym. Sci., Polym. Phys. Ed., 15, 1329 (1977).